

Polymer supported vanadium and molybdenum complexes as potential catalysts for the oxidation and oxidative bromination of organic substrates

Mannar R. Maurya,^{*a} Umesh Kumar^a and P. Manikandan^b

Received 19th January 2006, Accepted 21st April 2006

First published as an Advance Article on the web 28th April 2006

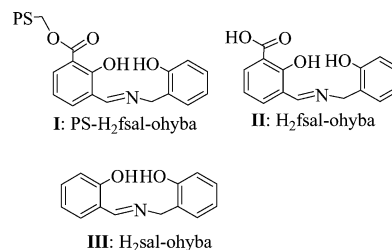
DOI: 10.1039/b600822d

The Schiff base (H₂fsal-ohyba) derived from 3-formylsalicylic acid and *o*-hydroxybenzylamine has been covalently bonded to chloromethylated polystyrene cross-linked with 5% divinylbenzene (abbreviated as PS-H₂fsal-ohyba, **I**). Treatment of [VO(acac)₂] with PS-H₂fsal-ohyba in dimethylformamide (DMF) gave the oxovanadium(IV) complex PS-[VO(fsalsal-ohyba)·DMF] (**1**). Complex **1** can be oxidized into the dioxovanadium(V) species, PS-K[VO₂(fsal-ohyba)] (**2**) on aerial oxidation in the presence of KOH or into the oxoperoxo species, PS-K[VO(O₂)(fsal-ohyba)] (**3**) in the presence of H₂O₂ and KOH in DMF suspension. Similarly, PS-[MoO₂(fsal-ohyba)·DMF] (**4**) has been isolated by the reaction of [MoO₂(acac)₂] with PS-H₂fsal-ohyba. All these complexes have been characterised by various techniques. These complexes catalyse the oxidation of styrene, ethylbenzene and phenol efficiently. Styrene gives five reaction products namely styrene oxide, benzaldehyde, 1-phenylethane-1,2-diol, benzoic acid and phenylacetaldehyde, while ethylbenzene gives benzaldehyde, phenyl acetic acid, styrene and 1-phenylethane-1,2-diol. The oxidation products of phenol are catechol and *p*-hydroquinone. These catalysts are also able to catalyse the oxidative bromination of salicylaldehyde to 5-bromosalicylaldehyde with *ca.* 80% selectively in the presence of aqueous 30% H₂O₂/KBr, a reaction similar to that exhibited by vanadate-dependent haloperoxidases. Their corresponding neat complexes have also been prepared and their catalytic activities have been compared.

Introduction

Discovery of vanadium(V) in the active site of vanadate-dependent haloperoxidases (V-HalPO) and its importance in catalytic reactions^{1–8} has stimulated research on the coordination chemistry of vanadium.⁹ These enzymes catalyse the oxidation of halides, by peroxide, to hypohalous acid which further halogenates hydrocarbons non-enzymatically.^{4,5} Many vanadium complexes show catalytic activity towards oxidative halogenations along with other oxidation reactions.^{10–13} However, these complexes generally decompose during the catalytic reaction and thus make their recovery from the catalytic reaction mixture difficult. Immobilization of these materials onto polymer supports through covalent attachment is one of the important means to solve this problem. Chloromethylated polystyrene cross-linked with divinylbenzene is one of the most widely employed macromolecular supports.^{14–17} These supported materials offer advantageous features of heterogeneous catalysis such as thermal stability, selectivity and recyclability to homogeneous systems and ease their separation from the reaction products also leading to operational flexibility.^{18,19}

Herein we report the preparation and characterisation of polymer-anchored oxovanadium(IV) and dioxovanadium(V) complexes of polymer-anchored ligand PS-H₂fsal-ohyba (**I**), Scheme 1. The corresponding neat complexes *i.e.* complexes of ligand H₂fsal-ohyba (**II**) and H₂sal-ohyba (**III**) have also been prepared. Spectral



Scheme 1

evidence has been presented for peroxide binding, in the presence of H₂O₂, to the vanadium centre. The catalytic potential of these complexes has been demonstrated by studying the oxidation of styrene, ethylbenzene and phenol. The ability of these complexes to mimic oxidative bromination in the presence of H₂O₂ and bromide has been demonstrated by considering salicylaldehyde as an example. The corresponding polymer-anchored as well as neat dioxomolybdenum(VI) complexes have also been prepared for comparison of their catalytic properties.

Experimental

Materials and methods

Chloromethylated polystyrene [18.9% Cl (5.3 mmol Cl per gram of resin)] cross-linked with 5% divinylbenzene was obtained as a gift from Thermax Limited, Pune, India. Analytical reagent grade V₂O₅, ethylbenzene (Loba Chemie, India), ammonium heptamolybdate, acetylacetone (E. Merck, India), aqueous 30% H₂O₂, salicylaldehyde, phenol (Ranbaxy, India), styrene (Acros

^aDepartment of Chemistry, Indian Institute of Technology Roorkee, Roorkee, 247667, India. E-mail: rkmanfey@iitr.ernet.in

^bCatalysis and Inorganic Chemistry Division, National Chemical Laboratory, Pune, 411008, India

organics, USA), and other chemicals were used as obtained. $\text{H}_2\text{fsal-ohyba}$,²⁰ $\text{H}_2\text{sal-ohyba}$,^{21,22} $[\text{VO}(\text{acac})_2]$,²³ $[\text{MoO}_2(\text{acac})_2]$,²⁴ 3-formylsalicylic acid,²⁵ and *o*-hydroxybenzylamine²⁶ were prepared according to the methods reported in the literature.

Elemental analyses of the ligands and complexes were obtained by an Elementar model Vario-EL-III. IR spectra were recorded as KBr pellets on a Nicolet NEXUS Aligent 1100 FT-IR spectrometer. Electronic spectra of the polymer-anchored compounds were recorded in Nujol on a Shimadzu 1601 UV-Vis spectrophotometer by a layering mull of the sample on the inside of one of the cuvettes while keeping the other one layered with Nujol as reference. Other ligands and complexes were recorded in methanol. ^1H NMR spectra were obtained on a Bruker 200, and ^{51}V NMR spectra on a Bruker Avance 400 MHz spectrometer at 94.73 MHz with common parameter settings. NMR spectra were recorded in DMSO-d_6 , and $\delta(^{51}\text{V})$ values are referenced relative to VOCl_3 as external standard. EPR spectra were recorded at room temperature on a Bruker EMX X-band spectrometer operating at 100 kHz field modulation at room temperature. The microwave frequency was calibrated using a frequency counter of the Microwave Bridge ER 041 XG-D. The Bruker Simfonia software package was used in the spectral simulations and to calculate hyperfine coupling constants. The magnetic susceptibilities of the oxovanadium(IV) complexes were measured at 298 K with a Vibrating Sample Magnetometer model 155, using nickel as standard. Diamagnetic corrections were carried out using Pascal's increments.²⁷ Thermogravimetric analyses of the complexes were carried out using a TG Stanton Redcroft STA 780 under oxygen atmosphere. Scanning electron micrographs (SEM) of catalysts were recorded on a Leo instrument model 435 VP. The samples were coated with a thin film of gold to prevent surface changing and to protect the surface material from thermal damage by the electron beam.

Preparation of ligand

Polymer anchored ligand, PS- $\text{H}_2\text{fsal-ohyba}$ I. Polymer-anchored ligand, PS- $\text{H}_2\text{fsal-ohyba}$ was prepared following the procedure developed by Syamal and Singh.²⁰ Chloromethylated polystyrene (3.0 g) was allowed to swell in DMF (30 ml) for 2 h. A solution of $\text{H}_2\text{fsal-ohyba}$ (12.2 g, 45 mmol) in DMF (40 ml) was added to the above suspension followed by triethylamine (4.50 g) in ethylacetate (100 ml). The reaction mixture was heated at 90 °C for 15 h with mechanical stirring in an oil bath. After cooling to room temperature, the yellow resins were filtered off, washed thoroughly with hot DMF followed by methanol and dried in an air oven at 120 °C.

Preparation of complexes

PS-[VO(*fsal-ohyba*)-DMF] 1. Polymer-anchored ligand PS- $\text{H}_2\text{fsal-ohyba}$ (1.50 g) was allowed to swell in DMF (25 ml) for 2 h. A solution of $[\text{VO}(\text{acac})_2]$ (5.30 g, 20 mmol) in 20 ml DMF was added to the above suspension and the reaction mixture was heated at 90 °C in an oil bath for 15 h with slow mechanical stirring. After cooling to ambient temperature, the dark green polymer-anchored complex was filtered off, washed with hot DMF followed by hot methanol and dried at 120 °C in an air oven.

PS-K[VO₂(*fsal-ohyba*)] 2. Complex 1 (1.5 g) was suspended in aqueous KOH (1.12 g, 20 mmol in 15 ml) and air was bubbled through the suspension for *ca.* 48 h. During this period the color of the beads slowly changed to dark red. They were filtered off, washed with water and dried at 120 °C in an air oven.

PS-K[VO(O₂)(*fsal-ohyba*)] 3. Complex 1 (1.5 g) was suspended in 15 ml water and to this KOH (0.56 g, 10 mmol) and 30% aqueous H_2O_2 (1.5 ml) were added and the suspended reaction mixture was stirred at room temperature. After *ca.* 10 h a further 1 ml of H_2O_2 was added and stirring continued for an additional 10 h. During this period the colour of the beads slowly changed to orange. They were filtered off, washed with H_2O and dried at room temperature over silica gel.

PS-[MoO₂(*fsal-ohyba*)-DMF] 4. This was prepared following the method reported by Syamal and Singh.²⁰ Polymer-anchored ligand PS- $\text{H}_2\text{fsal-ohyba}$ (2.0 g) was allowed to swell in DMF (20 ml) for 2 h. $[\text{MoO}_2(\text{acac})_2]$ (7.28 g, 22 mmol) was added to the above suspension and the reaction mixture was heated at 90 °C in an oil bath for 10 h with stirring. After cooling to ambient temperature, the orange-red polymer-anchored complex 4 was filtered off, washed with hot DMF followed by hot methanol and dried at 120 °C in an air oven.

[VO(*fsal-ohyba*)] 5. A stirred solution of $\text{H}_2\text{fsal-ohyba}$ (1.355 g, 5 mmol) in dry methanol (50 ml) was treated with $[\text{VO}(\text{acac})_2]$ (1.33 g, 5 mmol) dissolved in dry methanol (25 ml) and the resulting reaction mixture was refluxed in an oil bath for 2 h. After cooling to *ca.* 10 °C overnight, a green precipitate of 5 was filtered off, washed with methanol and dried *in vacuo*. Yield 80%.

[K[VO(O)₂(*fsal-ohyba*)] 6. Complex 5 (0.672 g, 2 mmol) was suspended in methanol (50 ml) and after addition of KOH (0.112 g, 2 mmol) and 30% H_2O_2 (2 ml) air was bubbled through for about 36 h with stirring. During this period, 0.5 ml portions of H_2O_2 were added *ca.* every 9 h and the green suspension slowly disappeared. After keeping the solution at 10 °C overnight the yellow solid that separated was filtered off, washed with cold methanol and dried *in vacuo*. Yield 63%.

[K(H₂O)] [VO₂(*fsal-ohyba*)] 7. A solution of PPh_3 (0.393 g, 1.5 mmol) in 10 ml of acetonitrile was added to 6 (0.407 g, 1 mmol) dissolved in 15 ml acetonitrile and the reaction mixture was refluxed on a water bath for 6 h. After cooling and reducing the volume of the solvent to *ca.* 5 ml it was kept at 10 °C overnight and a greenish solid separated out. This was filtered off, washed with cold methanol and dried *in vacuo*. Yield 87%.

[MoO₂(*fsal-ohyba*)-MeOH] 8. To a stirred solution of $\text{H}_2\text{fsal-ohyba}$ (0.271 g, 1 mmol) in 30 ml of methanol was added $[\text{MoO}_2(\text{acac})_2]$ (0.33 g, 1 mmol) with vigorous shaking and a clear solution was obtained. After filtering, the solution was refluxed on a water bath for 6 h and thereafter the volume was reduced to *ca.* 10 ml and kept in a refrigerator overnight. The yellow solid which separated was filtered off, washed with methanol and dried *in vacuo*. Yield 75%.

[VO(*sal-ohyba*)] 9. This complex was prepared analogously to 5, replacing $\text{H}_2\text{fsal-ohyba}$ with $\text{H}_2\text{sal-ohyba}$. After 5 h of

refluxing, the precipitated blackish solid was filtered off, washed with methanol and dried *in vacuo* over silica gel. Yield 71%.

[K(H₂O)]VO₂(sal-ohyba) 10. Complex **9** (0.292 g, 1 mmol) was suspended in methanol (40 ml) and after addition of KOH (0.561 g, 1 mmol) air was bubbled through the suspension for 2 days with occasional shaking. During this period, the blackish suspension slowly dissolved. After filtering and reducing the volume of the solvent to *ca.* 5 ml, it was kept at room temperature where a brownish-yellow solid slowly precipitated. This was filtered off, washed with methanol and dried *in vacuo*. Yield: 69%.

[MoO₂(sal-ohyba)·MeOH] 11. Complex **11** was prepared as reported previously.²¹ Yield 60%.

Reactivity of PS-K[VO(O₂)(fsal-ohyba)] with PPh₃

Peroxo complex **3** (1.5 g) was suspended in 20 ml of acetonitrile and after adding PPh₃ (5.25 g, 20 mmol), the suspended mixture was heated at 80 °C for 12 h with slow stirring. During this period the colour of the beads slowly changed to dark red. They were filtered off, washed with acetonitrile and dried at 120 °C in an air oven. Spectral data of the obtained complex matched well with **2**.

Catalytic reactions

Oxidation of styrene. Oxidation of styrene was carried out in a 50 ml reaction flask fitted with a water condenser. The catalysts were swelled in acetonitrile for 2 h prior to use. In a typical oxidation reaction, styrene (1.04 g, 10 mmol) and aqueous 30% H₂O₂ (2.27 g, 20 mmol) were mixed in 20 ml acetonitrile and the reaction mixture was heated to 80 °C. An appropriate catalyst (0.040 g) was added to the reaction mixture and stirred for 6 h. The progress of the reaction was monitored by withdrawing reaction samples at different time intervals and analysing them quantitatively by gas chromatography. The identities of the products were confirmed by GC-MS (Perkin-Elmer, Clarus 500). The effect of various parameters such as temperature, amount of oxidant and catalyst were checked to optimise the conditions for the best catalyst performance.

Oxidation of ethylbenzene. Polymer anchored catalysts after swelling in acetonitrile as stated above, were used for the oxidation of ethylbenzene. Ethylbenzene (0.42 g, 4 mmol), 30% aqueous H₂O₂ (0.906 g, 8 mmol) and catalyst (0.050 g) in 10 ml acetonitrile were heated at 80 °C and the reaction was monitored as mentioned above. Various parameters such as amount of oxidant and catalyst, and temperature were considered in order to study their effect on the reaction products. However, the basic procedure was the same as outlined above.

Oxidation of phenol. In a typical experiment, phenol (4.7 g, 0.05 mol) and 30% aqueous H₂O₂ (5.67 g, 0.05 mol) were suspended in 2 ml of acetonitrile and the reaction mixture was heated in an oil bath with stirring at *ca.* 80 °C. When an appropriate catalyst (0.025 g), after swelling in acetonitrile, was charged into it, the reaction was considered to begin. The reaction products were

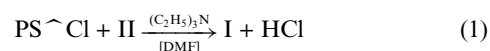
analysed using gas chromatography after specific time intervals by withdrawing a small aliquot.

Oxidative bromination of salicylaldehyde. In a typical reaction, aqueous 30% H₂O₂ (2.27 g, 20 mmol) was added to the mixture of salicylaldehyde (1.22 g, 10 mmol) and KBr (2.38 g, 20 mmol) taken in 10 ml of water. An appropriate catalyst (30 mg) and H₂SO₄ (0.490 g, 5 mmol) were added to it and the reaction mixture was stirred at room temperature. An additional 15 mmol H₂SO₄ was added to the reaction mixture in three equal portions at 20 min intervals under continuous stirring. After 2 h, the separated white product was filtered off, washed with water followed by diethyl ether and dried in air. The crude mass was dissolved in CH₂Cl₂; the insoluble solid, if any, was filtered off and the solvent evaporated. A CH₂Cl₂ solution of this material was subjected to gas chromatography and the identity of the products was confirmed by GC-MS.

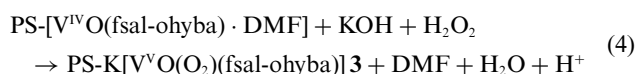
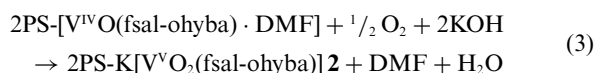
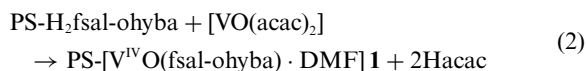
Results and discussion

Synthesis, reactivity and solid state characteristics

The chloromethylated polystyrene, cross-linked with 5% divinylbenzene, reacts with ligand **II** in DMF in presence of triethylamine to give polymer-anchored ligand PS-H₂fsal-ohyba (**I**). Carrying out the reaction at 90 °C was required for effective anchoring. At this temperature the ligand did not decompose due to its high melting point. Miller and Sherrington have used refluxing toluene to carry out the anchoring of organic ligands to chloromethylated polystyrene.²⁸ During this process the –COOH group of 3-formylsalicylic acid reacts with the –CH₂Cl group as shown in eqn (1) (for **I** and **II**, see Scheme 1). The remaining chlorine content of 1.5% (0.42 mmol Cl per gram of resin) in the anchored ligand suggests roughly 92% loading of the ligand.

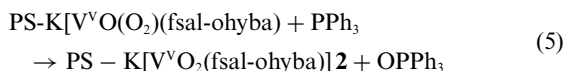


The anchored ligand on reaction with [VO(acac)₂] in DMF gave the oxovanadium(IV) complex PS-[VO(fsalsal-ohyba)·DMF] (**1**). On aerial oxidation of **1** in the presence of KOH in DMF, the dioxovanadium(V) complex PS-K[VO₂(fsal-ohyba)] (**2**) was obtained. Similarly, addition of H₂O₂ to PS-[VO(fsalsal-ohyba)·DMF] suspended in acetonitrile in the presence of KOH gave the oxomonoperoxo complex PS-K[VO(O₂)(fsal-ohyba)] (**3**). A change in the colour of the beads can also be visualized during the reactions. Eqn (2), (3) and (4) represent the synthetic procedures.



The dioxo complex **2** can also be obtained by the reaction of peroxo complex **3** with PPh₃; eqn (5). During this process PPh₃

abstracts one of the oxygen atoms from the peroxo group of **3**.



The reaction between $[\text{MoO}_2(\text{acac})_2]$ and PS- $\text{H}_2\text{fsal-ohyba}$ is straight forward, where acetylacetonate groups are replaced by a strong ONO donor ligand to give PS- $[\text{MoO}_2(\text{fsal-ohyba})\cdot\text{DMF}]$ (**4**). Similarly, reaction of $[\text{VO}(\text{acac})_2]$ with an equimolar amount of **II** and **III** in refluxing methanol yielded the oxovanadium(IV) complexes $[\text{VO}(\text{fsal-ohyba})]$ (**5**) and $[\text{VO}(\text{sal-ohyba})]$ (**9**), respectively. These complexes exhibit effective magnetic moments of 1.41 (for **5**) and $1.12 \mu_{\text{B}}$ (for **9**) at 298 K, which is subnormal for d^1 ($S = 1/2$) systems. Syamal and Kale²⁹ have suggested antiferromagnetic exchange in **9** on the basis of low temperature magnetic susceptibility studies. We studied the magnetic susceptibility of **5** as a function of temperature in the 298–90 K range. The magnetic moment shows the dependence of $\chi_{\text{M}}^{\text{corr}}$ on temperature and the observed magnetic moment values vary in the range $1.41\text{--}0.84 \mu_{\text{B}}$. The Curie–Weiss plot [$1/\chi_{\text{M}}^{\text{corr}}$ vs. T] is a straight line with a Weiss constant of *ca.* -20 indicating an antiferromagnetic interaction possibly through dimerisation.^{29,30}

Treatment of a methanolic solution of **5** with H_2O_2 in the presence of an equimolar amount of KOH gave oxo-monoperoxo complex, **6**. This is slightly stable and loses oxygen slowly at room temperature in a week period to give the respective dioxo complex. The formation of the oxo-monoperoxo vanadium(V) complex, $[\text{VO}(\text{O}_2)(\text{fsal-ohyba})]^-$ has also been established by electronic absorption spectroscopy in methanol. In a typical reaction 10 ml of *ca.* 1×10^{-4} M solution of **5** was treated with one drop portions of 30% H_2O_2 dissolved in methanol and the resulting spectral changes are presented in Fig. 1. Thus, the intensity of the 397 nm band increases quickly with the addition of the first two drops of H_2O_2 solution. Further addition of H_2O_2 causes a shift of this band to 392 nm along with a partial decrease in intensity. The 336 nm band does not change its position but undergoes an increase in intensity, while the band at 253 nm broadens initially and later disappears with an increase in intensity. The final spectral pattern is very similar to that obtained for the isolated peroxo complex **6** in methanol.

Aerial oxidation of a methanolic solution of **9** in the presence of one equivalent of KOH, gave dioxovanadium(V) complex **10** while

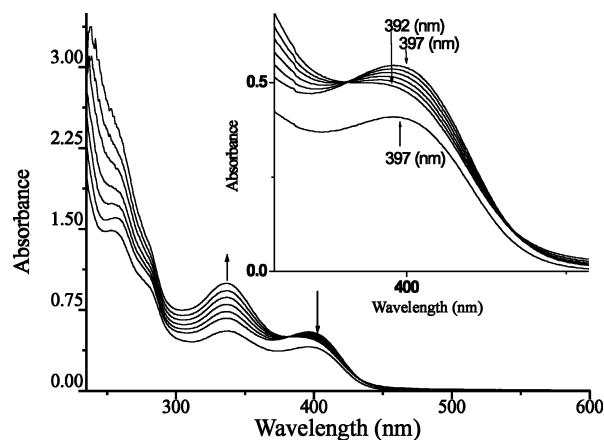
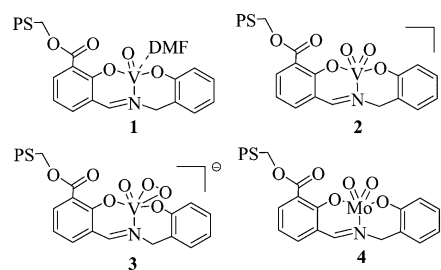


Fig. 1 Titration of $[\text{VO}(\text{fsal-ohyba})]$ (**5**) with 30% H_2O_2 ; the spectra were recorded after the successive addition of 1-drop portions of H_2O_2 dissolved in methanol to 10 ml of *ca.* 10^{-4} M solution of **5** in methanol.

7 could not be obtained under the above conditions. However, this could be isolated through an oxygen transfer reaction between **6** and PPh_3 (eqn (5)). Physico-chemical data of the isolated complexes are presented in Table 1.

Scheme 2 presents the proposed structures of the polymer-anchored complexes prepared in this contribution. These are based on various physico-chemical studies (*vide infra*) of neat as well as polymer-anchored complexes. A similar dioxovanadium(V) complex, *e.g.* $[\text{VO}_2(\text{sal-ea})]^-$ ($\text{H}_2\text{sal-ea}$ = Schiff base derived from salicylaldehyde and 2-amino-2-methylpropane-1-ol) having a



Scheme 2

Table 1 Physical and analytical data

Compound	Colour	Found (Calc.) (%)			
		C	H	N	V/Mo ^a
PS- $\text{H}_2\text{fsal-ohyba}$, 1	Yellow	75.44	7.42	2.50	—
PS- $[\text{VO}(\text{fsal-ohyba})\cdot\text{DMF}]$, 1	Greenish-black	68.03	6.91	2.17	6.2
PS- $\text{K}[\text{VO}_2(\text{fsal-ohyba})]$, 2	Dark red	67.34	6.82	2.07	5.7
PS- $\text{K}[\text{VO}(\text{O}_2)(\text{fsal-ohyba})]$, 3	Orange	64.57	6.71	2.05	5.7
PS- $[\text{MoO}_2(\text{fsal-ohyba})\cdot\text{DMF}]$, 4	Orange-red-red	64.74	6.59	2.11	6.9
$[\text{VO}(\text{fsal-ohyba})]$, 5	Green	53.38 (53.59)	3.31 (3.30)	4.12 (4.17)	14.9 (15.15)
$\text{K}[\text{VO}(\text{O}_2)(\text{fsal-ohyba})]$, 6	Yellow	44.16 (44.23)	2.81 (2.72)	3.29 (3.44)	12.3 (12.52)
$[\text{K}(\text{H}_2\text{O})][\text{VO}_2(\text{fsal-ohyba})]$, 7	Greenish-yellow	44.13 (44.01)	3.18 (3.20)	3.31 (3.42)	12.1 (12.46)
$[\text{MoO}_2(\text{fsal-ohyba})\cdot\text{MeOH}]$, 8	Yellow	44.43 (44.55)	3.64 (3.51)	3.17 (3.25)	22.1 (22.72)
$[\text{VO}(\text{sal-ohyba})]$, 9	Blackish	57.48 (57.53)	3.82 (3.80)	4.65 (4.80)	16.8 (17.45)
$[\text{K}(\text{H}_2\text{O})][\text{VO}_2(\text{sal-ohyba})]$, 10	Brown-yellow	46.59 (46.03)	3.11 (3.59)	3.96 (3.84)	13.5 (13.96)
$[\text{MoO}_2(\text{sal-ohyba})\cdot\text{MeOH}]$, 11	Yellow	46.32 (46.51)	4.03 (3.91)	3.51 (3.62)	24.80 (25.30)

^a Calculated from TGA data.

cis-VO₂ structure has been structurally characterised.^{9,31} The structure of [MoO₂(sal-ohyba)·MeOH] has already been confirmed by a single crystal X-ray study.^{22,32}

Scanning electron micrograph

Scanning electron micrographs (SEM) for a single bead of pure chloromethylated polystyrene, polymer-anchored ligand and the vanadium complexes were recorded to observe the morphological changes. Some of these images are reproduced in Fig. 2. As expected the pure polystyrene bead has a smooth and flat surface while the anchored ligand and complexes show a very slight roughening of the top layer. This roughening is relatively larger in the complex possibly due to the interaction of vanadium with the anchored ligand that resulted in the formation of a complex with a fixed geometry. Accurate information on the morphological changes in terms of exact orientation of ligands coordinated to the metal ion has not been possible due to poor loading of the metal complex.

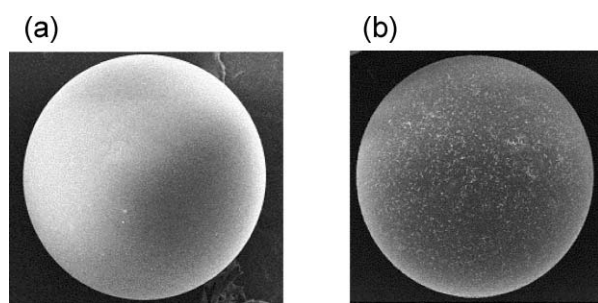


Fig. 2 Scanning electron micrographs (SEM) of (a) PS-H₂fsal-ohyba (**1**) and (b) PS-K[VO₂(fsalsal-ohyba)] (**2**); magnification ~200×.

TGA study

Thermogravimetric analysis under an oxygen atmosphere shows the good stability of polymer-anchored complex **2** up to *ca.* 250 °C and thereafter decomposes in several steps. Complexes **1** and **4** start losing weight at *ca.* 175 °C, possibly due to the loss of coordinated DMF followed by weight loss in multiple steps as noted above. Quantitative measurement of weight loss at various stages was not possible due to their overlapping nature. However, the stability of the final residues at *ca.* 650 °C suggests the formation of V₂O₃ (10.1% for **1**), KVO₃ (15.4% for **2**) or MoO₃ (10.35% for **4**). The peroxo complex **3**, as expected, starts decomposing at *ca.* 100 °C due to rupture of the peroxo group followed by decomposition of the organic moiety to give KVO₃ (15.4%) as the final product at *ca.* 650 °C. Estimation of final residues was helpful in approximating the percentage of metal ions in the polymer-anchored complexes.

IR spectral study

A partial list of IR spectral data of the polymer-anchored ligand and complexes are listed in Table 2. Complex **1** exhibits a sharp band at 970 cm⁻¹ due to $\nu(\text{V}=\text{O})$ while dioxo complex **2** exhibits two such bands at 927 and 888 cm⁻¹ corresponding to $\nu_{\text{antisym}}(\text{O}=\text{V}=\text{O})$ and $\nu_{\text{sym}}(\text{O}=\text{V}=\text{O})$ modes, respectively.⁹ The peroxo complex shows three IR active vibrational modes asso-

Table 2 IR spectral data (cm⁻¹)

Compound ^a	$\nu(\text{C}=\text{O})$	$\nu(\text{C}=\text{N})$	$\nu(\text{M}=\text{O})$ (M = V, Mo)
I	1685	1611	—
1	1671	1600	970
2	1660	1605	927, 888
3^b	1668	1606	932
4	1673	1604	953, 906
II	1668	1612	—
5	1661	1601	988
6^c	1661	1601	946
7	1661	1600	969, 918
8	1672	1603	942, 907
III	—	1656	—
9	—	1630	913
10	—	1638	896, 860
11	—	1632	933, 911

^a For details see Table 1. ^b Bands due to peroxo group: 860, 773, 591 cm⁻¹.

^c Bands due to peroxo group: 885, 761, 621 cm⁻¹.

ciated with the {V(O₂)}²⁺ moiety, namely the symmetric V(O₂) stretch (ν_2) at 591 cm⁻¹, the antisymmetric V(O₂) (ν_3) at 773 cm⁻¹, and the O–O (ν_1) stretch at 860 cm⁻¹, characteristic of η^2 -coordination of the peroxo group.³³ In addition, this displays the $\nu(\text{V}=\text{O})$ mode at 932 cm⁻¹. The dioxomolybdenum(VI) complex **4** exhibits two bands at 953 and 906 cm⁻¹ due to its *cis*-[MoO₂]²⁺ structure.³⁴ As shown in Table 2, the corresponding neat (oxo, dioxo and peroxo) complexes also exhibit characteristic bands well within the expected region.

The polymer-anchored ligand exhibits a sharp band at 1685 cm⁻¹ due to the $\nu(\text{C}=\text{O})$ of the carboxylic group. Existence of this band suggests covalent bond formation between the ligand and the polymer through a carboxylic acid group. A strong band appearing at 1611 cm⁻¹ due to the $\nu(\text{C}=\text{N})$ of the ligand undergoes a negative shift by 5–11 cm⁻¹ in the complexes. This observation suggests the coordination of the azomethine nitrogen atom to the metal ion. The coordination of phenolic oxygen could not be assigned unequivocally in most complexes because of the appearance of a weak broad band in the *ca.* 3400 cm⁻¹ region. However, the absence of such band in **9** suggests the coordination of phenolic oxygen to the vanadium. Neat vanadium and molybdenum complexes display spectral patterns very close to those above and are similar to those reported in literature.^{20,22,29}

Electronic spectral study

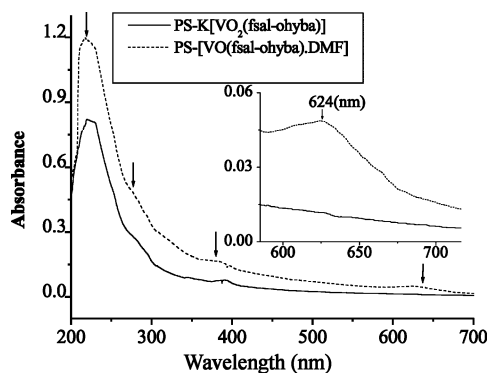
The electronic spectral studies of ligands H₂sal-ohyba, H₂fsal-ohyba and PS-H₂fsal-ohyba, and their metal complexes have been described earlier in detail.^{20–22} The electronic spectral patterns exhibited by the ligands and complexes in the UV region are similar to those observed earlier (Table 3).^{20–22} In addition, oxovanadium(IV) complexes, [VO(sal-ohyba)], [VO(fsalsal-ohyba)] and PS-[VO(fsalsal-ohyba)·DMF] display one weak shoulder between 517 and 630 nm due to a d-d transition. A band appearing at *ca.* 400 nm in neat dioxovanadium(V) and peroxo-oxovanadium(V) complexes is assigned to a ligand-to-metal charge transfer band (LMCT). In some dioxovanadium(V) and both dioxomolybdenum(VI) complexes, the $n \rightarrow \pi^*$ and LMCT bands merge together and appear as a broad band at *ca.* 400 nm. As a LMCT band generally requires a high concentration of metal complexes, such a band could not be located in the polymer-anchored dioxovanadium(V)

Table 3 Electronic spectral data

Compound ^a (solvent)	λ_{\max}/nm
I (Nujol)	296, 216
1 (Nujol)	624, 321, 281, 224
2 (Nujol)	292.5, 275, 229
3 (Nujol)	295, 280, 225
4 (Nujol)	304, 271, 219, 207
II (methanol)	401, 260, 279(sh), 221, 208
5 (methanol)	630, 397, 336, 253, 214
6 (methanol)	398, 341, 258, 206.5
7 (methanol)	401, 342, 255, 208
8 (methanol)	347(br), 281, 209
III (methanol)	314, 277, 255, 212
9 (methanol)	517, 496.5, 351.5, 206
10 (methanol)	406.5, 325, 281, 254, 213.5
11 (methanol)	360, 305, 272,

^a For details see Table 1.

and dioxomolybdenum(vi) complexes. The electronic spectra of some anchored and neat complexes are reproduced in Fig. 3 and 4, respectively.

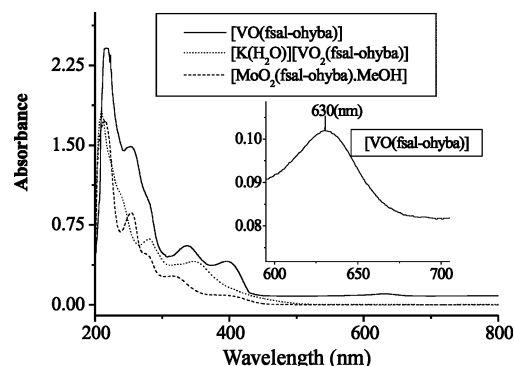
**Fig. 3** Electronic spectra of polymer-anchored complexes.

¹H and ⁵¹V NMR studies

The coordinating modes of the ligands H₂fsal-ohyba and H₂sal-ohyba were also confirmed by comparing ¹H NMR spectra of the ligands with the neat complexes **6**, **7**, **8**, **10** and **11**. The relevant spectroscopic data are collected in Table 4. A broad signal appearing at 12.50–13.24 ppm in the ligands, due to a phenolic proton, disappears in the spectra of the complexes and this suggests the coordination of a phenolic oxygen atom. A significant down field shift ($\Delta\delta = 0.33$ – 1.39 ppm) of the azomethine ($-\text{CH}=\text{N}-$) signal in the complexes with respect to the corresponding ligand demonstrates the coordination of the azomethine

Table 4 ¹H NMR and ⁵¹V NMR spectral data (δ in ppm)

Compound	–OH	–CH=N–	–CH ₂	Aromatic H	⁵¹ V NMR
H ₂ fsal-ohyba	13.24(br)	10.17(s)	4.87(s)	8.80–6.60(m)	
K[VO(O ₂)(fsal-ohyba)], 6	—	10.73(s)	4.86(s)	7.90–6.67(m)	–528.5
[K(H ₂ O)][VO ₂ (fsal-ohyba)], 7	—	10.60(s)	4.86(s)	7.92–6.67(m)	–515.9
[MoO ₂ (fsal-ohyba)·MeOH], 8	—	10.50(s)	4.86(s)	7.94–6.65(m)	
H ₂ sal-ohyba	12.50(br)	9.01(s)	4.70(s)	8.60–6.65(m)	
[K(H ₂ O)][VO ₂ (sal-ohyba)], 10	—	10.40(s)	4.77(s)	8.88–6.61(m)	–521.0
MoO ₂ (sal-ohyba)·MeOH], 11	—	10.30(s)	4.77(s)	8.85–6.60(m)	

**Fig. 4** Electronic spectra of free complexes.

nitrogen atom. The methylene and aromatic protons appear at almost the same position in the ligands as in their complexes. All these data are consistent with the conclusion drawn from the IR spectral studies and support the dibasic tridentate ONO coordination mode of the ligands.

The $\delta(^{51}\text{V})$ values of the dioxovanadium(v) complexes (also presented in Table 4) display one strong resonance at -515.9 (in **7**) and at -521.0 ppm (in **10**) in DMSO- d_6 ; an expected value for dioxovanadium(v) complexes having mixed O/N coordinating atoms.^{35–37} The resonances are somewhat broadened due to quadrupolar interactions (^{51}V : nuclear spin = $7/2$, quadrupole moment = $-0.05 \times 10^{-28} \text{ m}^2$); the line width at half height is approximately 200 Hz, which is still considered comparatively narrow in ^{51}V NMR spectroscopy.^{36,37} The peroxovanadium(v) complex **6** displays a signal at -528.5 ppm. This upfield shift with respect to dioxovanadium(v) complexes is commonly observed as an oxo group is replaced by the side-on coordinated peroxo group.³⁸

EPR studies

Room temperature X-band EPR spectra of the polymer anchored complex, PS-[VO(fsal-ohyba)·DMF] and the neat complex [VO(fsal-ohyba)] are reproduced in Fig. 5. The EPR spectrum of the polymer anchored sample (Fig. 5a) is characteristic of monomeric V(IV) complexes with an axial pattern. The hyperfine features are well resolved in both parallel and perpendicular regions. The resolved EPR pattern suggests that the vanadium centers are well separated. The simulation of the EPR spectrum was carried out in order to extract the Hamiltonian parameters. Accordingly, the values are: $g_{\parallel} = 1.946$, $A_{\parallel} = 184 (\pm 2) \text{ G}$, $g_{\perp} = 1.985$, $A_{\perp} = 65 (\pm 2) \text{ G}$ where the microwave frequency was 9.4458 GHz. The hyperfine lines are due to the interaction of an unpaired electron of a V(IV) center with its own nucleus (V , $I = 7/2$). The

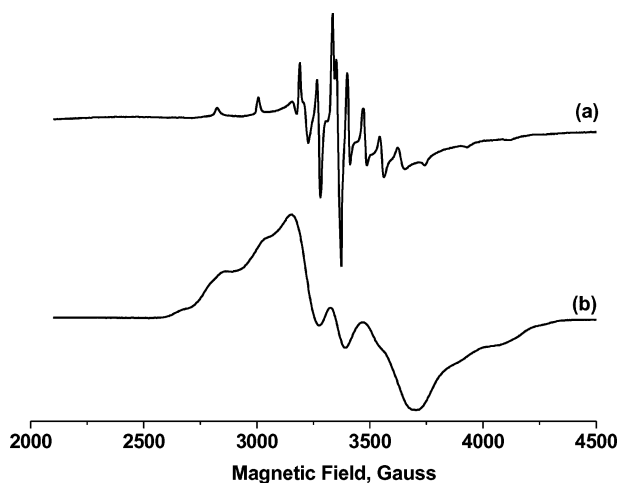


Fig. 5 X-Band EPR spectra of PS-[VO(fsal-ohyba)-DMF] (a) and [VO(fsal-ohyba)] (b).

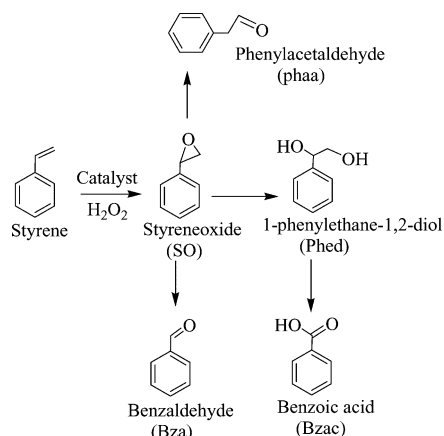
above parameters possibly indicate that the geometry is distorted square pyramidal where the V=O bond is along the *z*-axis.

The EPR spectrum of the neat complex **5**, unlike the polymer anchored complex **1**, exhibits broad signals as shown in Fig. 5(b). The spectrum could not be simulated with a monomeric V(IV) model, in combination with magnetic susceptibility data, indicating the presence of a dimeric species with a magnetic superexchange interaction between the two V(IV) centers. Such a dimeric structure has been confirmed *e.g.* for [VO(sal-*ea*)]₂ (H₂sal-*ea* = Schiff base derived from salicylaldehyde and 2-aminoethanol) by a X-ray single crystal study.³⁹

Catalytic activity study

The catalytic potential of polymer-anchored as well as neat complexes were studied for the oxidation of styrene, ethylbenzene and phenol, and for the oxidative bromination of salicylaldehyde.

Oxidation of styrene. Oxidation of styrene catalysed by polymer-anchored complexes, PS-[VO(fsal-ohyba)-DMF], PS-K[VO₂(fsal-ohyba)] and PS-[MoO₂(fsal-ohyba)-DMF] gave styrene oxide, benzaldehyde, benzoic acid, phenylacetic acid and 1-phenylethane-1,2-diol as mentioned in Scheme 3. These reaction



Scheme 3

products are common and have also been identified previously by others.⁴⁰

Amongst these catalysts, PS-K[VO₂(fsal-ohyba)] was taken as a representative and three different parameters *viz.* amount of H₂O₂ (moles of H₂O₂ per mole of styrene), and catalyst, and temperature of the reaction mixture were varied to obtain suitable reaction conditions for the maximum oxidation of styrene. For three different molar ratios (1 : 1.5, 1 : 2 and 1 : 3 of styrene to aqueous 30% H₂O₂), the amount of styrene (1.04 g, 10 mmol) and catalyst (0.040 g) in 10 ml of CH₃CN at 80 °C were fixed and the results after 6 h of contact time were analysed. As illustrated in Fig. 6, the oxidation of styrene improved from 40.2% to 79.7% on increasing from 1 : 1.5 to 1 : 2 (styrene to H₂O₂) molar ratios. This oxidation remained nearly constant on further increasing the molar ratio to 1 : 3, which suggests that a large amount of oxidant is not an essential condition to improve the oxidation of styrene. Similarly for three different amounts (*viz.* 0.030 g, 0.040 g and 0.070 g) of catalyst and styrene to H₂O₂ ratio of 1 : 2 under the above reaction conditions, 0.030 g catalyst gave only 45.2% conversion while 0.040 g and 0.070 g catalyst have shown a maximum conversion of 79.7 and 81.3%, respectively; Fig. 7. However, at the expense of H₂O₂, 0.040 g catalyst can be considered sufficient enough to carry out the reaction. Further, the turnover

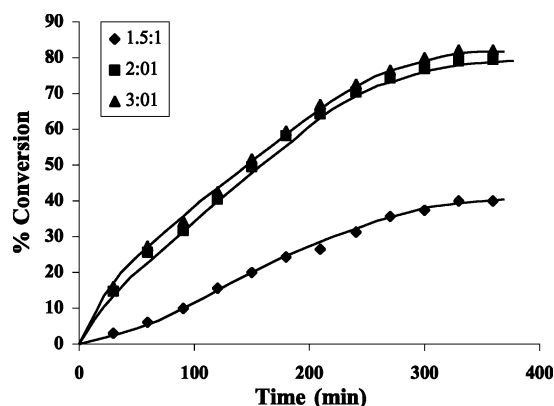


Fig. 6 Effect of amount of H₂O₂ on the oxidation of styrene. Reaction conditions: styrene (1.04 g, 10 mmol), PS-K[VO₂(fsal-ohyba)] (0.040 g), CH₃CN (10 ml) and temp. (80 °C).

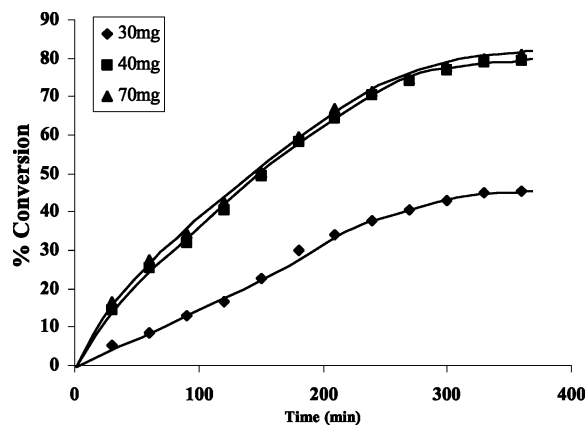


Fig. 7 Effect of amount of catalyst PS-K[VO₂(fsal-ohyba)] on the oxidation of styrene. Reaction conditions: styrene (1.04 g, 10 mmol), H₂O₂ (2.27 g, 20 mmol), CH₃CN (10 ml) and temp. (80 °C).

rates (TOF h^{-1} = moles of substrate converted per mole of catalyst per hour) is also higher for 0.040 g catalyst to achieve 79.7% conversion of styrene. The temperature of the reaction mixture has also influenced the performance of the catalyst. Amongst three different temperatures (60, 70 and 80 °C), running the reaction at 80 °C gave much better conversion; Fig. 8. Moreover, the time required to achieve the maximum conversion was also reduced on carrying out the reaction at 80 °C.

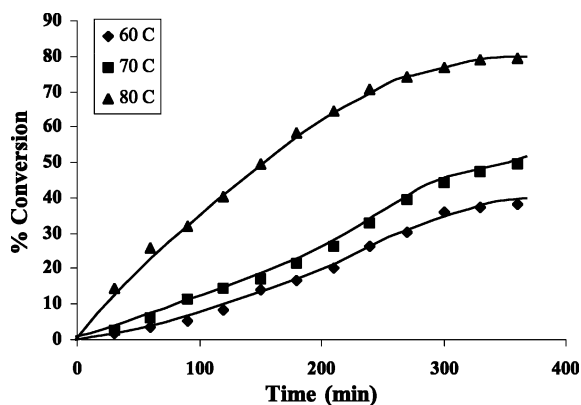


Fig. 8 Effect of temperature on oxidation of styrene. Reaction conditions: styrene (1.04 g, 10 mmol), PS-K[VO₂(fsal-ohyba)] (0.040 g), H₂O₂ (2.27 g, 20 mmol) and CH₃CN (10 ml).

Other catalysts *e.g.* PS-[VO(fsal-ohyba)-DMF] and PS-[MoO₂(fsal-ohyba)-DMF] were also tested under the above optimized reaction conditions. Thus, for 10 mmol of substrate, 20 mmol aqueous 30% H₂O₂ and 0.040 g catalyst were taken in 10 ml of CH₃CN and the reaction was carried out at 80 °C. The results presented in Table 5 show that PS-K[VO₂(fsal-ohyba)] exhibits better catalytic activity (79.7% conversion of styrene) than PS-[VO(fsal-ohyba)-DMF]; here only 73.2% conversion was achieved, though one should expect nearly the same conversion as both would form peroxo species easily in the presence of H₂O₂ (*vide supra*). The PS-[MoO₂(sal-ohyba)-DMF], on the other hand, gave only 17.5% conversion. The difficulty in transferring oxygen from the intermediate peroxo complex, PS-[MoO(O₂)(sal-ohyba)], formed by the reaction between PS-[MoO₂(sal-ohyba)-DMF] and H₂O₂ may be the possible reason for the poor oxidation ability of the catalyst. No significant improvement in conversion was noted beyond 6 h of reaction time in all cases.

We have compared the catalytic activity of these polymer-anchored complexes with their respective neat ones. The conversion percentage for each catalyst as a function of time is presented in Fig. 9, Table 5 presents selectivity details of various products obtained after 6 h of reaction time. For 0.040 g each of the neat vanadium complex and keeping the other reaction conditions fixed as above, the obtained percentage conversion varies in the range 53.3 to 63.7% with the order: [K(H₂O)]VO₂(fsal-ohyba) (63.7%) > [K(H₂O)]VO₂(sal-ohyba) (60.5%) > [VO(fsal-ohyba)] (57.2%) > [VO(sal-ohyba)] (53.3%). Thus, the catalytic performances of the neat complexes are also good. However, the TOF values are much less in comparison to the polymeric ones. Moreover, easy recovery of the anchored catalyst, no leaching and recycle ability make them better over the neat complexes. Similarly, the immobilized dioxomolybdenum(vi) complex is a better catalyst over the neat [MoO₂(fsal-ohyba)-MeOH]. Independent of catalyst, the product selectivity follows the order: benzaldehyde > 1-phenylethane-1,2-diol > benzoic acid > phenylacetaldehyde > styrene oxide. The formation of benzaldehyde in highest yield is understandable because the styrene oxide formed in the first step may convert into benzaldehyde by a nucleophilic attack of H₂O₂ on styrene oxide followed by cleavage of the intermediate hydroperoxystyrene; Scheme 4. Benzaldehyde formation may also be facilitated by direct oxidative cleavage of the styrene side chain double bond *via* a radical mechanism.⁴⁰ Other products *e.g.* benzoic acid formation through benzaldehyde is rather slow in all reactions.

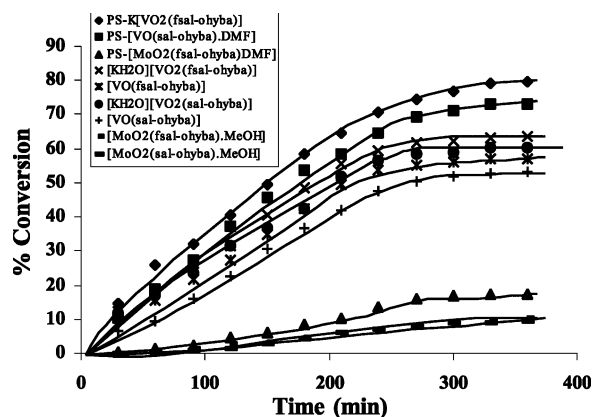
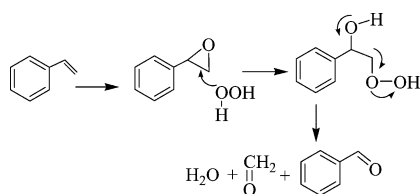


Fig. 9 Catalytic comparison of catalysts for the oxidation of styrene. Reaction conditions: styrene (1.04 g, 10 mmol), catalyst (0.040 g), H₂O₂ (1.27 g, 20 mmol), CH₃CN (10 ml), temp. (80 °C).

Table 5 Percent conversion of styrene and selectivity of various oxidation products

Catalyst	Conversion (%)	TOF/h ⁻¹	Selectivity ^a (%)					
			SO	Phaa	Bza	Bzac	Phed	Others
PS-K[VO ₂ (fsal-ohyba)]	79.7	29.5	3.54	2.97	60.65	9.82	20.61	2.45
PS-[VO(fsal-ohyba)-DMF]	73.2	25.1	3.21	4.15	60.67	8.46	18.83	4.68
PS-[MoO ₂ (fsal-ohyba)-DMF]	17.5	10.1	4.19	4.82	64.01	8.67	16.42	1.89
[VO(fsal-ohyba)]	57.2	8.2	4.27	5.39	53.36	11.51	21.16	4.31
[K(H ₂ O)]VO ₂ (fsal-ohyba)	63.7	10.8	3.82	4.22	57.31	9.63	20.5	4.52
[VO(sal-ohyba)]	53.3	6.7	3.86	3.77	58.17	9.91	19.91	4.38
[K(H ₂ O)]VO ₂ (sal-ohyba)	60.5	10.5	3.22	3.92	57.59	10.82	20.34	4.11
[MoO ₂ (fsal-ohyba)-MeOH]	10.2	1.8	3.69	4.28	60.66	9.43	18.09	3.85
[MoO ₂ (sal-ohyba)-MeOH]	9.6	1.5	2.95	4.53	61.29	10.53	17.72	2.98

^a SO = styrene epoxide, Phaa = phenylacetaldehyde, Bza = benzaldehyde, Bzac = benzoic acid, Phed = 1-phenylethane-1,2-diol.



Scheme 4

Similarly, the formation of phenylacetaldehyde, a product formed by isomerisation of styrene oxide is less in all cases. Water present in H_2O_2 is probably responsible for hydrolysis of styrene oxide to 1-phenylethane-1,2-diol to some extent.

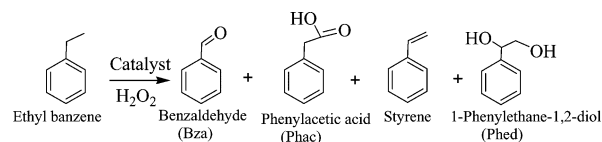
The oxidation of styrene at the side chain of industrially important fine chemicals has also been obtained previously using different types of catalysts. Mainly homogeneous catalysts such as cobalt chloride,⁴¹ $[\text{Mn}^{\text{III}}(\text{salen})]$ ($\text{H}_2\text{salen} = N,N'$ -bis(salicyliden)ethane-1,2-diamine),⁴² $[\text{Cr}^{\text{III}}(\text{dpa})(\text{dipy}/\text{o phen})\text{Cl}]$, $[\text{Fe}^{\text{III}}(\text{dpa})(\text{dipy}/\text{o phen})\text{Cl}]$ ($\text{H}_2\text{dpa} =$ pyridine-2,6-dicarboxylic, $\text{dipy} =$ 2,2'-dipyridyl, $\text{o phen} =$ 1,10, phenanthroline),⁴³ mixed-metal carboxylate,⁴⁴ Mn^{III} -complexes attached to crown ethers,⁴⁵ vanadium peroxy complexes,⁴⁶ and metalloporphyrins,⁴⁷ and heterogeneous catalysts such as heteropolytungstates,⁴⁸ nano-sized spinel type mixed metal oxides,⁴⁹ zeolites,⁵⁰ metal complexes encapsulated in zeolites or anchored to mesoporous materials,⁵¹ metal containing TM-MCM-41 and TM-MCM-48 (TM = Al, Ti, V, Cr, Mn, Fe, Co and Ni),⁵² titanium containing molecular sieves (TS-1,⁵³ BTS,⁵⁴ Ti-MCM-41⁴⁰) and silica⁵⁵ have been used for the oxidation of styrene. The literature, however, contains very limited citations on polymer supported catalysts for the oxidation of styrene.^{56,57}

Within the polymer supported catalysts, the catalytic activity of these anchored vanadium complexes is better than that reported for the similar polymer-anchored PS- $[\text{VO}(\text{hmbzm})_2]$ [where PS-Hhmbzm = polymer-anchored 2-(α -hydroxymethyl)benzimidazole] under similar reaction conditions.⁵⁶ Here, the highest selectivity of benzaldehyde (78%) and lowest of styrene oxide (4.4%) were maintained while conversion was limited to 48%. For the polymer-anchored peroxovanadium(V) complex PS-K $[\text{VO}(\text{O}_2)_2(2\text{-pybzm})]$ [where 2-pybzm = 2-(2-pyridyl)benzimidazole], the percent conversion as well as the selectivity of all five products (Scheme 3) were nearly same.⁵⁸ Oxidation of styrene catalysed by a poly(maleic acid-co-styrene)-triruthenium cluster gave three major products: benzaldehyde (65.4%), phenylacetaldehyde (15.3%) and acetophenone (11.5%). As molecular oxygen was used as oxidant, the Wacker-type oxidation of styrene was suggested to follow for the formation of these products.⁵⁷ The neat vanadium complex $[\text{VO}(\text{salphen})]$ [where $\text{H}_2\text{salphen} = N,N'$ -bis(salicyliden)phenyl-1,2-diamine] exhibits only 10.7% conversion using 70% *tert*-butylhydroperoxide and among the only two products identified, the selectivity of benzaldehyde is 32.2 and of styrene oxide is 9.4%. Encapsulation in zeolite-Y reverses this selectivity along with 34.8% conversion. This conversion was further improved to 40.6% on anchoring $[\text{VO}(\text{salphen})]$ to Al-MCM-41 with an improvement in selectivity to 45.0% towards the formation of styrene oxide.^{51a} Catalytic activity of $[\text{Mn}(\text{salen})]^+$ encapsulated in zeolite-Y has been tested using molecular oxygen as oxidant in excess *tert*-butylhydroperoxide as initiator. While activity of the catalyst is about 30%, the selectivity of the formation

of benzoic acid is highest (67.9%) followed by benzaldehyde (29.7%), and selectivity of styrene oxide and phenylacetaldehyde is 0.6 and 1.6%. The highest selectivity of benzoic acid is clearly due to further oxidation of benzaldehyde.⁴²

Oxidation of ethylbenzene. Selective oxidation of ethylbenzene to acetophenone has been considered an important chemical reaction because of its use as an intermediate in pharmaceuticals, resins, alcohols, esters, aldehydes, and tear gas. For the oxidation of ethylbenzene, homogeneous (*e.g.* metal acetylacetonates,⁵⁹ $[\text{Co}(2\text{-pyridinecarboxamide})_3]$,⁶⁰ metalloporphyrins,⁶¹ macrocyclic complexes⁶² *etc.*) as well as heterogeneous catalysts (*e.g.* metal salt or complex supported on alumina/silica,⁶³ heteropolyacids⁶⁴ M-APO-11 (M = Co, Mn and V),⁶⁵ Mn-MCM-41,⁶⁶ polymer-anchored complexes,^{56,67} zeolite encapsulated metal complexes⁶⁸ *etc.*) have been employed. Mostly molecular oxygen has been used as oxidant^{59–68} and there are only limited reports where *tert*-butyl hydroperoxide/ H_2O_2 has been used as oxidant.^{56,67,68} With mild oxidants usually acetophenone is obtained as the major product while strong oxidants give several oxidized products.

We have used polymer-anchored complexes to catalyse the oxidation of ethylbenzene, by H_2O_2 , to give benzaldehyde, phenylacetic acid, styrene and 1-phenylethane-1,2-diol as shown in Scheme 5. Reaction conditions have also been optimised for the maximum oxidation of ethylbenzene by varying the amount of oxidant (moles of H_2O_2 per mole of ethylbenzene), catalyst and temperature of the reaction considering PS-K $[\text{VO}_2(\text{fsal-ohyba})]$ as a representative catalyst.



Scheme 5

The effect of temperature on the oxidation of ethylbenzene was studied at three different temperatures (*viz.* 50, 60 and 80 °C) while keeping ethylbenzene (0.424 g, 4 mmol), aqueous 30% H_2O_2 (0.906 g, 8 mmol), and catalyst (0.050 g) in 10 ml of CH_3CN . It is clear from the profile presented in Fig. 10 as a function of time that performance of the catalyst is much better at 80 °C compared to

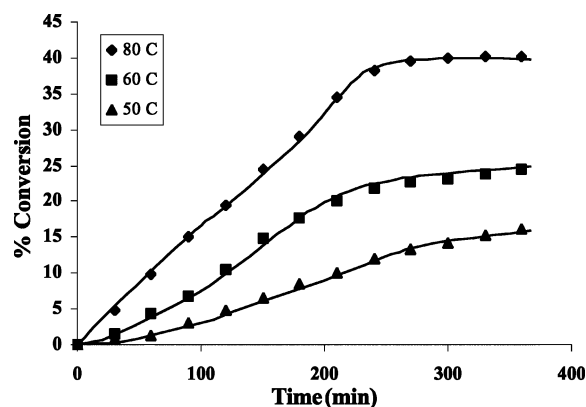


Fig. 10 Effect of temperature on the oxidation of ethylbenzene. Reaction conditions: ethylbenzene (0.424 g, 4 mmol), H_2O_2 (0.906 g, 8 mmol), PS-K $[\text{VO}_2(\text{fsal-ohyba})]$ (0.050 g) and CH_3CN (10 ml).

50 and 60 °C along with the maximum conversion in considerably less time. Thus, a minimum of 80 °C is the required temperature to cross the energy barrier to get maximum conversion of substrate.

The influence of H₂O₂ concentration on the oxidation of ethylbenzene as a function of time has been studied considering ethylbenzene : H₂O₂ molar ratios of 1 : 1, 1 : 2 and 1 : 3, and the results are illustrated in Fig. 11 as a function of time. For a fixed amount of ethylbenzene (0.424 g, 4 mmol), catalyst (0.050 g) and CH₃CN (10 ml), the conversion of ethylbenzene was 22.6% in 6 h of reaction time at 80 °C for the substrate to H₂O₂ molar ratio of 1 : 1. Increasing this ratio to 1 : 2 increases the conversion to 40% and reaches completion within 6 h while further enhancement of H₂O₂ hardly affects the conversion. The effect of amount of catalyst on the oxidation of ethylbenzene is illustrated in Fig. 12. It is clear from the plot that reaction proceeds slowly and gives only 19.2% conversion with 0.030 g of catalyst, ethylbenzene (0.424 g, 4 mmol) and H₂O₂ (0.906 g, 8 mmol) in 10 ml of CH₃CN after 6 h of reaction time. Increasing the catalyst amount to 0.050 g, improves this conversion to 40% within 6 h of reaction time. Further increment of catalyst amount has no further effect on the oxidation of ethylbenzene.

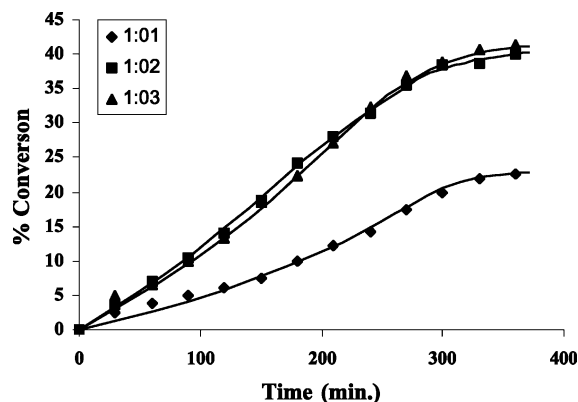


Fig. 11 Effect of amount of H₂O₂ on the oxidation of ethylbenzene. Reaction conditions: ethylbenzene (0.424 g, 4 mmol), PS-K[VO₂(fsal-ohyba)] (0.050 g), CH₃CN (10 ml) and temperature (80 °C).

Table 6 presents the results of ethylbenzene oxidation under optimised reaction conditions after 6 h of reaction time while Fig. 13 presents the conversion as a function of time. Catalysts PS-K[VO₂(fsal-ohyba)] and PS-[VO(fs al-ohyba)-DMF] show

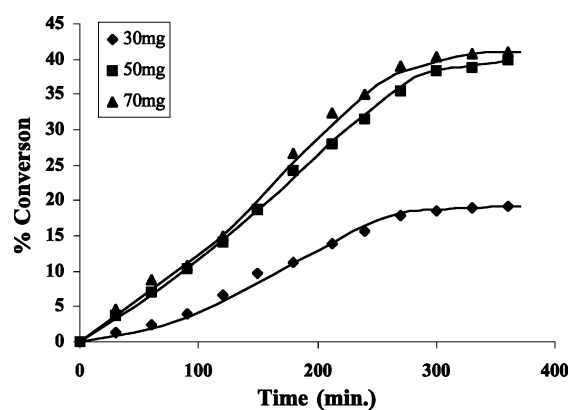


Fig. 12 Effect of amount of catalyst on the oxidation of ethylbenzene. Reaction conditions: ethylbenzene (0.424 g, 4 mmol), H₂O₂ (0.906 g, 8 mmol), CH₃CN (10 ml) and temperature (80 °C).

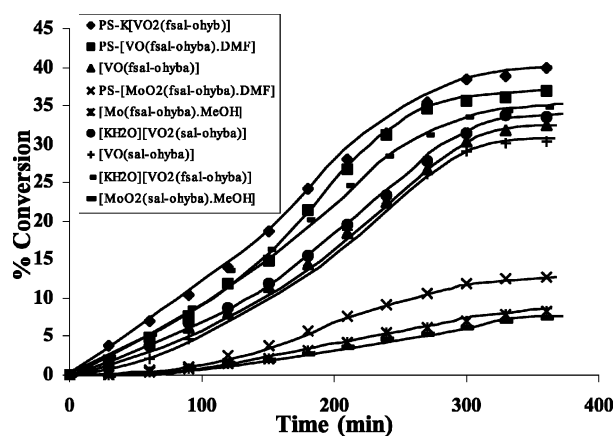


Fig. 13 Comparison of catalytic potential of catalysts on the oxidation of ethylbenzene under optimised conditions. Reaction conditions: ethylbenzene (0.424 g, 4 mmol), H₂O₂ (0.906 g, 8 mmol), catalyst (0.050 g), CH₃CN (10 ml) and temperature (80 °C).

very comparative results and give 40 and 36.9% conversion, respectively, while PS-[MoO₂(fsal-ohyba)·DMF] shows very poor performance, here only 12.8% conversion was achieved. The products formed are independent of catalyst and follow the order: benzaldehyde > phenylacetic acid > styrene > 1-phenylethane-1,2-diol. A very small amount of unidentified product was also noticed (see Table 6). No significant improvement in the

Table 6 Effect of oxidant on percentage conversion of ethylbenzene and selectivity of various oxidation products

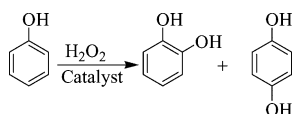
Catalyst	Conversion (%)	TOF/h ⁻¹	Selectivity ^a (%)				
			Phac	Bza	Styrene	Phed	Others
PS-K[VO ₂ (fsal-ohyba)]	40.0	4.7	7.61	87.51	2.13	1.21	1.54
PS-[VO(fs al-ohyba)-DMF]	36.9	4.1	7.05	85.42	4.37	1.13	2.23
PS-{{[MoO ₂ (fsal-ohyba)·DMF]	12.83	2.4	8.64	83.84	3.52	1.19	2.93
[VO(fs al-ohyba)]	32.5	1.5	9.81	82.18	4.36	1.08	2.47
[K(H ₂ O)][VO ₂ (fsal-ohyba)]	34.8	1.9	8.28	85.77	2.86	1.29	1.8
[VO(sal-ohyba)]	30.4	1.2	8.59	84.62	2.91	1.36	2.52
[K(H ₂ O)][VO ₂ (sal-ohyba)]	33.6	1.9	8.75	83.49	3.61	1.32	2.83
[MoO ₂ (fsal-ohyba)·MeOH]	8.2	0.5	8.26	82.52	3.94	1.21	4.07
[MoO ₂ (sal-ohyba)·MeOH]	7.5	0.4	8.61	81.49	4.27	1.35	4.28

^a Phac = phenylacetic acid, Bza = benzoic acid, Phed = 1-phenylethane-1,2-diol.

oxidation of ethylbenzene was observed beyond 6 h of reaction time. Neat complex [VO(fsal-ohyba)] shows 32.5% conversion of ethylbenzene when 0.050 g of it was used under the above optimised conditions. However, the turnover rates per hour are very low compared to the respective polymer-anchored catalyst. Again, performance of [MoO₂(fsal-ohyba)·MeOH] is very poor.

The catalytic potentials of these polymer-anchored complexes compare well with other polymer supported catalysts, e.g. PS-[VO(hmbmz)₂].⁵⁶ However, the latter is more selective towards the formation of acetophenone under similar conditions. At the same time, with *ca.* 28% conversion PS-par-Cu (par = 4-(2-pyridylazo)resorcinol)⁶⁷ is less selective towards the formation of acetophenone (38.3%) and more towards benzylalcohol (57.2%). The zeolite framework in zeolite encapsulated complexes has influence on the oxidation products of ethylbenzene in that using TBHP or H₂O₂ as oxidant, acetophenone was always obtained as the major product along with other minor products.⁶⁸ In the polymer-anchored catalysts reported here, oxidation of ethylbenzene does not stop at acetophenone but proceeds further to give several oxidation products, Table 6.

Oxidation of phenol. Liquid phase oxidation of phenol using simple oxidants such as O₂ and H₂O₂ has been reported using different types of heterogeneous catalyst. For example, polymeric coordination complexes,⁶⁹ polymer-anchored complexes,⁵⁸ metal complexes encapsulated in the super cages of zeolites,⁷⁰ *etc.* are well documented in the literature. Molecular sieve based catalysts, TS-1 and TS-2 have been commercialized for the oxidation of phenol using H₂O₂ as oxidant.⁷¹ We have studied the oxidation of phenol catalysed by polymer-anchored as well as neat complexes using H₂O₂ as an oxidant in CH₃CN. Only two major products, *viz.* catechol and *p*-hydroquinone as shown in Scheme 6 were identified from the reaction mixture. These are the expected products according to the directing effect of the phenolic OH group.



Scheme 6

In order to achieve suitable reaction conditions for the maximum oxidation of phenol as well as better selectivity for the formation of catechol we have studied the effect of amount of catalyst, effect of H₂O₂ concentration (moles of H₂O₂ per mole of phenol) and effect of temperature using PS-K[VO₂(fsal-ohyba)] as a representative catalyst.

The effect of H₂O₂ concentration on the oxidation of phenol is illustrated in Fig. 14. For three different molar ratios of H₂O₂ (*viz.* 50, 70 and 100 mmol), the amount of phenol (4.7 g, 50 mmol) and catalyst (0.025 g) were fixed in 2 ml of CH₃CN and the reaction was carried out at 80 °C. It is clear from the plots that a H₂O₂ to phenol ratio of 1 : 1 results in about 21% conversion in 6 h of reaction time. The other two concentrations (*i.e.* 1.4 : 1, and 2 : 1) performed better but gave comparable phenol conversions of 37.3 and 39.7%. However, in terms of the selectivity of H₂O₂, the 1.4 : 1 ratio would be a suitable oxidant to phenol ratio for better performance of the catalyst. Similarly out of three different catalyst weights (0.015,

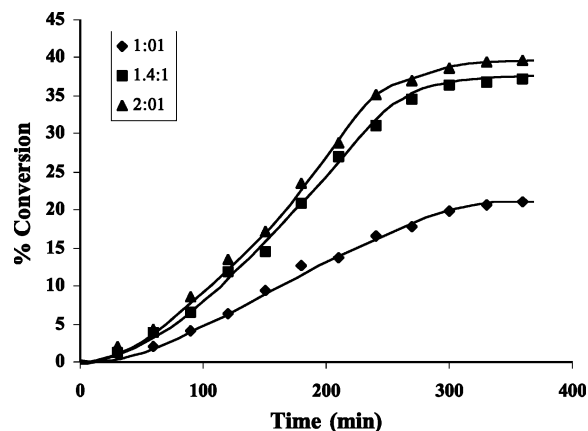


Fig. 14 Effect of H₂O₂ concentration on the oxidation of phenol. Reaction conditions: phenol (4.7 g, 50 mmol), PS-K[VO₂(fsal-ohyba)] (0.025 g), CH₃CN (2 ml) and temperature (80 °C).

0.025 and 0.040 g) for a fixed amount of phenol (4.7 g, 0.05 mol) and oxidant (7.93 g, 70 mmol) in 2 ml of CH₃CN, only 16.5% oxidation of phenol with 0.015 g catalyst was achieved at 80 °C in 6 h of reaction time. However, increments of catalyst amounting to 0.025 g showed significant change and conversion reached 37.3% within 6 h of reaction time. Further increments of catalyst hardly improve the oxidation. Fig. 15 presents this effect as a function of time. This has been interpreted in terms of the thermodynamic and mass transfer limitations at higher reaction rates. Running the reaction at various temperatures while considering a fixed amount of phenol (4.7 g, 50 mmol), H₂O₂ (7.93 g, 70 mmol), catalyst (0.025 g) and CH₃CN (2 ml) has shown a considerable effect on the oxidation of phenol. As shown in Fig. 16 at least 80 °C is the required temperature to supply sufficient energy to reach the energy barrier of phenol conversion.

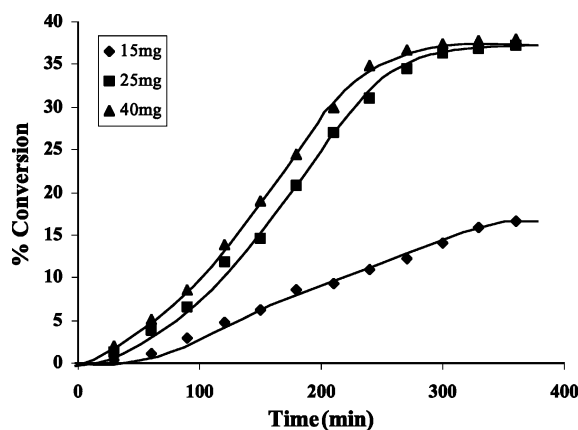


Fig. 15 Effect of amount of catalyst on the oxidation of phenol. Reaction conditions: phenol (4.7 g, 50 mmol), H₂O₂ (7.93 g, 70 mmol), CH₃CN (2 ml) and temperature (80 °C).

Thus, under the optimised conditions (*i.e.* 50 mmol substrate, 70 mmol 30% aqueous H₂O₂, 0.025 g catalyst, 2 ml CH₃CN and 80 °C reaction temperature), the performance of all catalysts were studied and the percentage of phenol oxidation plotted as a function of time are presented in Fig. 17. All catalysts acquired a steady state in *ca.* 6 h of contact time and only

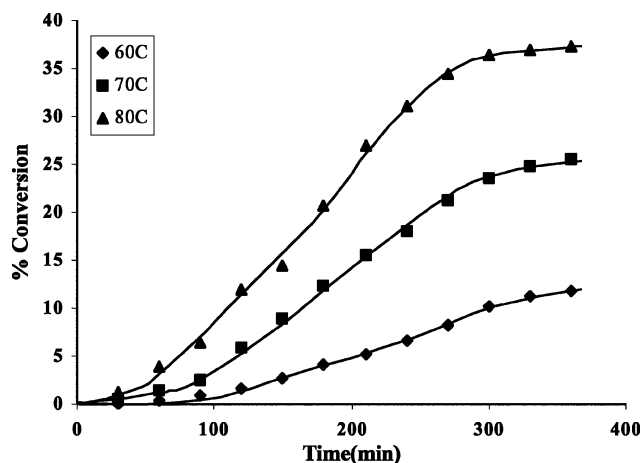


Fig. 16 Effect of temperature on the oxidation of phenol. Reaction conditions: phenol (4.7 g, 50 mmol), PS-K[VO₂(fsal-ohyba)] (0.025 g), H₂O₂ (7.93 g, 70 mmol) and CH₃CN (2 ml).

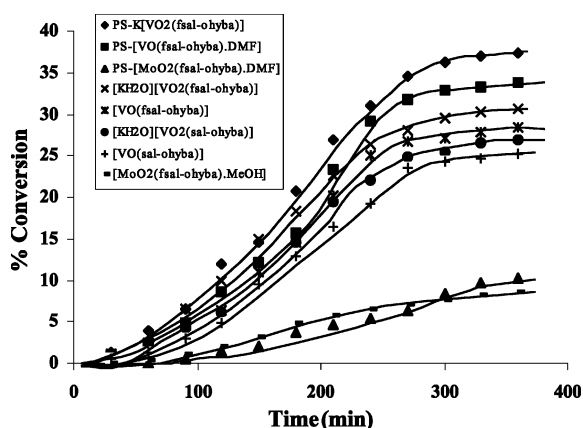


Fig. 17 Comparison of the catalytic activity of various catalysts on the oxidation of phenol under optimized condition. Reaction conditions: phenol (4.7 g, 50 mmol), catalyst (0.025 g), H₂O₂ (7.93 g, 70 mmol) and CH₃CN (2 ml) and temperature (80 °C).

minor changes either in conversion or selectivity of the product formation were observed beyond 6 h of contact time. Amongst the polymer-anchored catalysts, the performance followed the order: PS-K[VO₂(fsal-ohyba)] (37.3%) > PS-[VO(fsal-ohyba)·DMF] (33.8%) > PS-[MoO₂(fsal-ohyba)·DMF] (10.3%). It seems that the dioxovanadium(v) complex is more able to form the peroxy complex easily followed by transfer of oxygen to the

substrate than the oxovanadium(IV) complex. The poor stability of the peroxovanadium(V) complex has an added advantage in improving the phenol oxidation while the dioxomolybdenum(VI) forms a stable peroxomolybdenum(VI) complex and hence has difficulty in transferring the oxygen to the substrate thereby resulting in a poor yield of the oxidised products.

Taking 0.025 g of neat complex and keeping the other reaction conditions fixed as above, the catalytic performances follow the order: [K(H₂O)][VO₂(fsal-ohyba)] (30.7%) > [VO(fsal-ohyba)] (28.5%) > [K(H₂O)][VO₂(salsal-ohyba)] (26.9%) > [VO(salsal-ohyba)] (25.3%) > [MoO₂(fsal-ohyba)·MeOH] (8.5%). Again the vanadium based complexes have a better performance than the neat molybdenum(VI) one. But the overall performances of the polymer-anchored complexes are better than the corresponding neat complexes. The turnover rates of the polymer-anchored complexes are also higher than the corresponding neat complexes.

The percentage of phenol oxidation and the selectivity of the catechol and *p*-hydroquinone formation along with the turnover frequency of different catalysts after 6 h of contact time are presented in Table 7. It is clear from the data that the selectivity of neat as well polymer-anchored complexes is better for catechol formation where it varies between 58.8 and 69.5% while the selectivity of *p*-hydroquinone formation is between 27.5 and 39.2%.

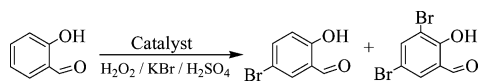
The catalytic performances of the polymer-anchored complexes reported here compare well with the data reported in the literature. For example, the reported conversions for polymer-anchored complex, PS-K[VO(O₂)(2-pybzmm)] (33.5%),⁵⁸ polymeric [-CH₂{VO(salen)}]_n (38.6%),⁶⁹ and zeolite encapsulated NH₄[VO₂(sal-inh)] (where H₂sal-inh = Schiff base derived from salicylaldehyde and isonicotinic acid hydrazide) (26.5%)^{70h} and [VO(salen)] (32.6%),^{70g} are close to that reported in Table 7. The data suggest equally good catalytic potential for these catalysts. However, their selectivity towards the formation of catechol vary in the order: [VO(salen)]-Y (92.7%) > [-CH₂{VO(salen)}]_n (92.5%) > NH₄[VO₂(sal-inh)]-Y (84.6%) > PS-K[VO(O₂)(2-pybzmm)]. A poor performance for all types of molybdenum based catalysts was always noted.

Oxidative bromination of salicylaldehyde. As mentioned in the Introduction, vanadium(V) complexes catalyse the oxidative bromination of organic substrates in the presence of H₂O₂ and bromide.^{10,12} Bromination of 1,3,5-trimethoxybenzene to 2-bromo-1,3,5-trimethoxybenzene catalysed by [VO(OEt)(EtOH)(sal-oap)] [H₂sal-oap = *N*-(2-hydroxyphenyl)salicylidenamine]¹⁰ and phenol red to bromophenol red by [VO(O₂)(H₂O)]⁺ species⁷² are worthy of mention here. During this process, vanadium reacts

Table 7 Percentage conversion of phenol along with TOF values and the selectivity of the products formed after 6 h of contact time

Catalyst	Phenol conversion (%)	TOF/h ⁻¹	Selectivity (%)	
			Catechol	<i>p</i> -Hydroquinone
PS-[VO(fsalsal-ohyba)·DMF]	33.8	92.7	69.5	27.5
PS-K[VO ₂ (fsalsal-ohyba)]	37.3	110.5	66.7	31.2
PS-[MoO ₂ (fsalsal-ohyba)·DMF]	10.3	47.6	58.8	39.2
[VO(fsalsal-ohyba)]	28.5	32.6	59.4	37.2
[K(H ₂ O)][VO ₂ (fsalsal-ohyba)]	30.7	42.8	55.2	42.5
[MoO ₂ (fsalsal-ohyba)·MeOH]	8.5	12.3	54.7	42.1
[VO(salsal-ohyba)]	25.3	35.8	61.9	34.2
[K(H ₂ O)][VO ₂ (salsal-ohyba)]	26.9	33.8	59.8	37.2

with 1 or 2 equivalents of H_2O_2 , forming oxo-monoperoxo, $[\text{VO}(\text{O}_2)^+]$ or oxo-diperoxo $[\text{VO}(\text{O}_2)_2^-]$ species, which ultimately oxidise bromide, possibly *via* a hydroperoxo intermediate. The oxidised bromine species (most likely HOBr) then brominates the substrate.¹ We have found that polymer-anchored complexes satisfactorily catalyse the oxidative bromination of salicylaldehyde to give 5-bromosalicylaldehyde and 3,5-dibromosalicylaldehyde using $\text{H}_2\text{O}_2/\text{KBr}$ in the presence of H_2SO_4 in aqueous solution; *cf.* Scheme 7.



Scheme 7

In order to achieve optimum conditions, PS-K[VO₂(sal-ohyba)] was studied in detail by varying parameters such as the volume of sulfuric acid and H_2O_2 at room temperature. Thus, for a fixed amount of salicylaldehyde (1.22 g, 10 mmol), catalyst (0.030 g), KBr (2.38 g, 20 mmol) in 10 ml of water at least 20 mmol of H_2SO_4 (1.96 g) and 20 mmol of H_2O_2 (2.27 g) were found to be sufficient to give maximum conversion. Using 30 mmol of acid under the above conditions gave only a marginal improvement in conversion. As the presence of acid may cause decomposition of the catalyst, the effect of acid on the rate of reaction was studied in detail under the above operating conditions. The results after 2 h of reaction time are illustrated in Fig. 18. It is clear from the figure that conversion of salicylaldehyde significantly improves from 40.5% to 75% with the increment of H_2SO_4 from 10 mmol to 30 mmol but it was necessary to add the acid in batches to prevent decomposition of the catalyst. Using 40 mmol H_2SO_4 (*i.e.* substrate to H_2SO_4 ratio = 1 : 4) causes lower conversion along with the decomposition of

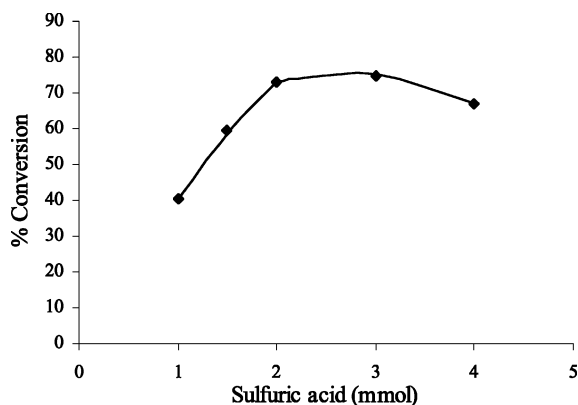


Fig. 18 Effect of H_2SO_4 on the oxidative bromination of salicylaldehyde.

catalyst. This was confirmed by comparing the IR spectrum of the recovered catalyst at each stage with that of a fresh sample.

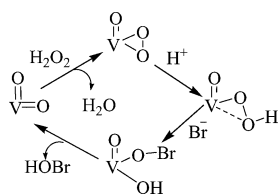
Under optimised reaction conditions (*i.e.* salicylaldehyde (1.22 g, 10 mmol), catalyst (30 mg), H_2O_2 (2.27 g, 20 mmol), H_2SO_4 (1.96 g, 20 mmol), KBr (2.38 g, 20 mmol) in 10 ml of water), the performance of the other polymer-anchored catalysts was also tested and the results along with turnover rate per hour and selectivity of the reaction products are summarised in Table 8. Approximately 73% conversion of salicylaldehyde with *ca.* 80% selectivity towards the formation of 5-bromosalicylaldehyde (5-Brsal) was achieved with vanadium based catalysts under optimised conditions. It is interesting to note that dioxomolybdenum(vi) complex, PS-[MoO₂(fsal-ohyba)·DMF] also mimics haloperoxidase activity in that 92% conversion of salicylaldehyde with a turnover rate per hour of 213.3 was achieved. Here the selectivity of 5-bromosalicylaldehyde is 83.4%. The performance of the previously reported polymer-anchored catalyst PS-[VO(hmbmz)₂] is better (100% conversion)⁵⁶ than the anchored vanadium and molybdenum complexes reported here. The reported turnover rates for zeolite-Y encapsulated dioxovanadium(v) complexes NH₄[VO₂(sal-inh)]-Y and NH₄[VO₂(sal-oap)]-Y (where H₂sal-oap = Schiff base derived from salicylaldehyde and *o*-aminophenol) are 52 and 67, respectively for similar catalytic reactions.^{70b} Simple vanadium complexes *e.g.* [K(H₂O)₂][VO₂(pydx-inh)] (H₂pydx-inh = Schiff base derived from pyridoxal and isonicotinic acid hydrazide) and [K(H₂O)][VO₂(sal-nah)] (H₂sal-nah = Schiff base derived from salicylaldehyde and isonicotinic acid hydrazide) have turnover rates per hour of about 5. In addition, they have a tendency towards slow decomposition during the catalytic reaction.⁷³ The performance of the polymeric oxovanadium(v) complexes of Schiff bases derived from 5,5'-methylenebis(salicylaldehyde) and diamines are relatively better but the turnover rates per hour is about 32.⁶⁹

The reaction mixture did not produce any brominated product in the absence of these catalysts. The recovered catalysts after regeneration with acetonitrile performed well with nearly the same percentage conversion and this suggests that these catalysts are recyclable.

Complex **1** generates oxoperoxo species (*vide supra*) and dioxovanadium(v) complexes are well known to form oxoperoxo species.⁷³ In the presence of H_2O_2 and acid, oxovanadium(IV) and dioxovanadium(v) may generate (proposed) intermediate hydroperoxo species,⁷³ which allow nucleophilic attack of the bromide,¹ followed by release of hypobromous acid, which then brominates an organic substrate. A catalytic cycle is proposed in Scheme 8. Dioxomolybdenum(vi) complexes may follow a similar mechanism. A hypobromite intermediate may also be involved, as proved by electrospray ionization mass spectra on model systems.⁷⁴

Table 8 Average percent conversion of salicylaldehyde along with TOF and product selectivity

Catalyst	Conversion (%)	TOF/h ⁻¹	Selectivity (%)		
			5-Brsal	3,5-diBrsal	Unidentified
PS-[VO(fsalsal-ohyba)·DMF]	73	100.0	81.36	15.82	2.82
PS-K[VO ₂ (fsal-ohyba)]	70	104.3	78.56	19.17	2.27
PS-[MoO ₂ (fsal-ohyba)·DMF]	92	213.3	83.44	14.03	2.53



Scheme 8

Test for recyclability and heterogeneity of the reaction

The recycle ability of the polymer-anchored catalysts **1**, **2** and **4** has been tested. The reaction mixture after a contact time of 6 h was filtered. The catalysts separated from the reaction mixture after the catalytic reaction in all three cases were washed with acetonitrile, dried and subjected to further catalytic reactions under similar conditions. No appreciable loss in the activity in all cases suggested that the metal complexes were interacting with the polystyrene and that the catalysts are active even after first cycle. During catalytic oxidation of styrene and ethylbenzene, the filtrate collected after separating the solid catalysts was placed into the reaction flask and the reaction was continued after adding fresh oxidant for another 2 h. The gas chromatographic analyses showed no further increment in the conversion. This confirms that the reaction did not proceed upon removal of the solid catalyst and hence the reaction was heterogeneous in nature.

Conclusion

Polymer-anchored oxovanadium(IV), dioxovanadium(V), oxoper-oxovanadium(V) and dioxomolybdenum(VI) complexes with polymer-anchored ligand PS-H₂fsal-ohyba having potential catalytic activities for the oxidation of styrene, ethylbenzene and phenol have been isolated and characterised. Independent of catalyst, the oxidation of styrene gives at least five different products with the following order of selectivity: benzaldehyde > 1-phenylethane-1,2-diol > benzoic acid > phenylacetaldehyde > styrene oxide. A maximum of 40% conversion of ethylbenzene was observed with PS-K[VO₂(fsal-ohyba)] which is followed by PS-[VO(fsal-ohyba)-DMF] with 36.9% conversion. Catalyst PS-[MoO₂(fsal-ohyba)-DMF] showed very poor results and only 12.8% conversion of ethylbenzene was achieved. The selectivity of various products follows the order: benzaldehyde > phenylacetic acid > styrene > 1-phenylethane-1,2-diol. Similarly, for phenol oxidation, PS-[VO(fsal-ohyba)-DMF] and PS-K[VO₂(fsal-ohyba)] are much better catalysts than PS-[MoO₂(fsal-ohyba)-DMF]. The selectivity of major product catechol is 58.8–69.5%, while of minor product *p*-hydroquinone is 27.5–39.2%. The catalytic activities of these complexes have also been compared with the corresponding free complexes and it is observed that some free complexes have comparable catalytic activity. However, the recycle ability and easy separation of the catalysts from the reaction mixture make polymer-anchored complexes better catalysts than neat ones. These polymer-anchored complexes also mimic the catalytic activity of vanadate-dependent haloperoxidases in that they catalyse the oxidative bromination of salicylaldehyde, by H₂O₂, in good yield to give 5-bromosalicylaldehyde and 3,5-dibromosalicylaldehyde. No decomposition or leaching of the catalysts during the catalytic

reactions suggests their heterogeneous nature. They are recyclable up to three cycles without significant loss in their catalytic activity.

Acknowledgements

This work was supported by the University Grant Commission, New Delhi. The authors are also thankful to Prof. Dr Dieter Rehder, Hamburg, Germany, for recording the ⁵¹V NMR spectra and Thermax Limited, Pune, India for providing chloromethylated polystyrene as a gift.

References

- (a) A. Butler, *Coord. Chem. Rev.*, 1999, **187**, 17; (b) A. Butler, in *Bioinorganic Catalysis*, ed. J. Reedijk and E. Bouwman, Marcel Dekker, New York, 2nd edn, 1999, ch. 5.
- M. Weyand, H. J. Hecht, M. Kieß, M. F. Liaud, H. Vilter and D. Schomburg, *J. Mol. Biol.*, 1999, **293**, 595.
- M. I. Isupov, A. R. Dalby, A. A. Brindley, Y. Izumi, T. Tanabe, G. N. Murshudov and J. A. Littlechild, *J. Mol. Biol.*, 2000, **299**, 1035.
- G. J. Colpas, B. J. Hamstra, J. W. Kampf and V. L. Pecoraro, *J. Am. Chem. Soc.*, 1996, **118**, 3469.
- B. J. Hamstra, G. J. Colpas and V. L. Pecoraro, *Inorg. Chem.*, 1998, **37**, 949.
- J. A. Littlechild and E. Garcia-Rodriguez, *Coord. Chem. Rev.*, 2003, **237**, 65.
- S. Macedo-Ribeiro, W. Hemrika, R. Renirie, R. Wever and A. Messerschmidt, *JBIC, J. Biol. Inorg. Chem.*, 1999, **209**, 209.
- A. Messerschmidt and R. Wever, *Proc. Natl. Acad. Sci. USA*, 1996, **93**, 392.
- M. R. Maurya, *Coord. Chem. Rev.*, 2003, **237**, 163.
- M. J. Clague, N. N. Keder and A. Butler, *Inorg. Chem.*, 1993, **32**, 4754.
- V. Conte, F. DiFuria and G. Licini, *Appl. Catal., A*, 1997, **157**, 335.
- A. G. J. Ligtenberg, R. Hage and B. L. Feringa, *Coord. Chem. Rev.*, 2003, **237**, 89.
- C. Bolm, *Coord. Chem. Rev.*, 2003, **237**, 245.
- R. S. Drago, J. Gaul, A. Zombeck and D. K. Straub, *J. Am. Chem. Soc.*, 1980, **102**, 1033.
- D. C. Sherrington, *Pure Appl. Chem.*, 1988, **60**, 401.
- (a) D. A. Annis and E. N. Jacobson, *J. Am. Chem. Soc.*, 1999, **121**, 4147; (b) J. K. Karjalainen, O. E. O. Hormi and D. C. Sherrington, *Molecules*, 1998, **3**, 51.
- (a) L. Canali and D. C. Sherrington, *Chem. Soc. Rev.*, 1999, **28**, 8; (b) D. C. Sherrington, *Catal. Today*, 2000, **57**, 87.
- B. Meunier, *Chem. Rev.*, 1992, **92**, 1411.
- D. C. Sherrington, in *Supported Reagents and Catalysts in Chemistry*, ed. B. K. Hodnett, A. P. Kybett, J. H. Clark and K. Smith, Royal Society of Chemistry, Cambridge, 1998, p. 220.
- A. Syamal and M. M. Singh, *Indian J. Chem., Sect. A*, 1992, **31**, 110.
- A. Syamal and M. R. Maurya, *Indian J. Chem., Sect. A*, 1986, **25**, 1152.
- M. R. Maurya, M. N. Jayaswal, V. G. Puranic, P. Chakravorty, S. Gopinathan and C. Gopinathan, *Polyhedron*, 1997, **23**, 3977.
- R. A. Row and M. M. Jones, *Inorg. Synth.*, 1957, **5**, 113.
- G. J.-J. Chen, J. W. McDonald and W. E. Newton, *Inorg. Chem.*, 1976, **15**, 2612.
- J. C. Duff and E. J. Bills, *J. Chem. Soc.*, 1923, 1987.
- L. C. Raiford and F. P. Clark, *J. Am. Chem. Soc.*, 1923, **45**, 1738.
- R. L. Dutta and A. Syamal, *Elements of Magnetochemistry*, Affiliated East-West Press, New Delhi, 2nd edn., 1993, p. 8.
- M. M. Miller and D. C. Sherrington, *J. Catal.*, 1995, **152**, 368.
- A. Syamal and K. S. Kale, *Inorg. Chem.*, 1979, **18**, 992.
- A. Syamal and K. S. Kale, *Indian J. Chem., Sect. A*, 1980, **19**, 225.
- G. Asgedom, A. Sreedhara, J. Kivikoski, J. Valkonen, E. Kolehmainen and C. P. Rao, *Inorg. Chem.*, 1996, **35**, 5674.
- C. Zhang, G. Rheinwald, V. Lozen, B. Wu, P.-G. Lassahn, H. Lang and C. Janiak, *Z. Anorg. Allg. Chem.*, 2002, **628**, 1259.
- A. D. Westland, F. Haque and J. M. Bouchard, *Inorg. Chem.*, 1980, **19**, 2255.
- A. Syamal and M. R. Maurya, *Coord. Chem. Rev.*, 1989, **95**, 83.

- 35 O. W. Howarth, *Prog. Nucl. Magn. Reson. Spectrosc.*, 1990, **22**, 453.
- 36 D. Rehder, C. Weidemann, A. Duch and W. Priebsch, *Inorg. Chem.*, 1988, **27**, 584.
- 37 D. Rehder, in *Transition Metal Nuclear Magnetic Resonance*, ed. P. S. Pregosin, Elsevier, New York, 1991, p. 1.
- 38 M. Cásny and D. Rehder, *Dalton Trans.*, 2004, 839.
- 39 C. J. Carrano, C. M. Nunn, R. Quan, J. A. Bonadies and V. L. Pecoraro, *Inorg. Chem.*, 1990, **29**, 944.
- 40 V. Hulea and E. Dumitriu, *Appl. Catal., A*, 2004, **277**, 99.
- 41 Y. H. Lin, I. D. Williams and P. Li, *Appl. Catal., A*, 1977, **150**, 221.
- 42 A. Zsigmond, A. Horváth and F. Notheisz, *J. Mol. Catal. A: Chem.*, 2001, **171**, 95.
- 43 P. B. Samnani, P. K. Bhattacharya, P. A. Ganeshpure, V. J. Koshy and S. Satish, *J. Mol. Catal. A: Chem.*, 1996, **110**, 89.
- 44 H. Kanai, H. Hayashi, T. Koike, M. Oshuga and M. Matsumoto, *J. Catal.*, 1992, **138**, 611.
- 45 W. Zeng, J. Li and S. Qin, *Inorg. Chem. Commun.*, 2006, **9**, 10.
- 46 B. M. Choudary and P. N. Reddy, *J. Mol. Catal. A: Chem.*, 1995, **103**, L1.
- 47 (a) S. S. Kurek, P. Michorczyk and A.-M. Balisz, *J. Mol. Catal. A: Chem.*, 2003, **194**, 237; (b) J.-Y. Liu, X.-F. Li, Y.-Z. Li, W.-B. Chang and A.-J. Huang, *J. Mol. Catal. A: Chem.*, 2002, **187**, 163.
- 48 (a) E. J. S. Reddy, U. R. Khire, P. Ratnasamy and R. B. Mitra, *J. Chem. Soc., Chem. Commun.*, 1992, 1234; (b) L. Xinrong, X. Jinyu, L. Huizhang, Y. Bin, J. Songlin and X. Gaoyang, *J. Mol. Catal. A: Chem.*, 2000, **161**, 163.
- 49 (a) N. Ma, Y. Yue, W. Hua and Z. Gao, *Appl. Catal., A*, 2003, **251**, 39; (b) D. Guin, B. Baruwati and S. V. Manorama, *J. Mol. Catal. A: Chem.*, 2005, **242**, 26.
- 50 L. M. Kustov, A. L. Tarasov, V. I. Bogdan, A. A. Tyrlov and J. W. Fulmer, *Catal. Today*, 2000, **61**, 123.
- 51 (a) T. Joseph, D. Srinivas, C. S. Gopinath and S. B. Halligudi, *Catal. Lett.*, 2002, **83**, 209; (b) S. N. Rao, K. N. Munsu and N. N. Rao, *J. Mol. Catal. A: Chem.*, 2000, **156**, 205.
- 52 (a) V. Parvulescu and B.-L. Su, *Catal. Today*, 2001, **69**, 315; (b) Q. Zhang, Y. Wang, S. Itsuki, T. Shishido and K. Takehira, *J. Mol. Catal. A: Chem.*, 2002, **188**, 189; (c) Y. Luo and J. Lin, *Mesoporous Microporous Mater.*, 2005, **86**, 23; (d) S. Gómez, L. J. Garces, J. Villegas, R. Ghosh, O. Giraldo and S. L. Suib, *J. Catal.*, 2005, **233**, 60.
- 53 (a) R. Irie, Y. Ito and T. Katsuki, *Synlett*, 1991, 265; (b) S. B. Kumar, S. P. Mirajkar, G. C. G. Pais, P. Kumar and R. Kumar, *J. Catal.*, 1995, **156**, 163; (c) M. A. Uguina, D. P. Serrano, R. Sanz, J. L. G. Fierro, M. López-Granados and R. Mariscal, *Catal. Today*, 2000, **61**, 263.
- 54 Z. Fu, D. Yin, D. Yin, Q. Li, L. Zhang and Y. Zhang, *Mesoporous Microporous Mater.*, 1999, **29**, 351.
- 55 Q. Yang, S. Wang, J. Lu, G. Guang, Z. Feng, Q. Xin and C. Li, *Appl. Catal., A*, 2000, **194–195**, 507.
- 56 M. R. Maurya, S. Sikarwar, T. Joseph, P. Manikandan and S. B. Halligudi, *React. Funct. Polym.*, 2005, **63**, 71.
- 57 C.-G. Jia, F.-Y. Jin, M.-Y. Huang and Y.-Y. Jiang, *React. Polym.*, 1994, **23**, 33.
- 58 M. R. Maurya, M. Kumar and S. Sikarwar, *React. Funct. Polym.*, 2006, in press.
- 59 (a) Y. Ishii, T. Iwahama, S. Sakaguchi, K. Nakayama and Y. Nishiyama, *J. Org. Chem.*, 1996, **61**, 4520; (b) R. Alcántara, L. Canoira, P. Guilherme-Joao and J. P. Pérez-Mendo, *Appl. Catal., A*, 2001, **218**, 269; (c) L. I. Matienko and L. A. Mosolova, *Kinetic Catal.*, 2005, **46**, 328.
- 60 J.-Y. Qi, H.-X. Ma, X.-J. Li, Z.-Y. Zhou, M. C. K. Choi, A. S. C. Chan and Q.-Y. Yang, *Chem. Commun.*, 2003, 1294.
- 61 (a) C. Guo, Q. Peng, Q. Liu and G. Jiang, *J. Mol. Catal. A: Chem.*, 2003, **192**, 295; (b) S. Evans and J. R. L. Smith, *J. Chem. Soc., Perkin Trans. 2*, 2001, 174; (c) S. Evans and J. R. L. Smith, *J. Chem. Soc., Perkin Trans. 2*, 2000, 1541.
- 62 L. I. Matienko and L. A. Mosolova, *Russ. Chem. Bull.*, 1997, **46**, 658.
- 63 (a) S. T. Man, C. Ramshaw, K. Scott, J. Clark, D. J. Macquarrie and R. Jachuck, *Org. Process Res. Dev.*, 2001, **5**, 204; (b) J. H. Clark, S. Evans and J. R. L. Smith, in *Supported Reagents and Catalysts in Chemistry*, ed. B. K. Hodnett, A. P. Kybett, J. H. Clark and K. Smith, Royal Society of Chemistry, Cambridge, 1998, p. 216; (c) I. C. Chisem, K. Martin, M. T. Shieh, J. Chisem, J. H. Clark, R. Jachuck, D. J. Macquarrie, J. Rafelt, C. Ramshaw and K. Scott, *Org. Process Res. Dev.*, 1997, **1**, 365.
- 64 Y. Yu, X. Li and S. Lin, *Huaxue Yanjiu Yu Yingyong*, 2000, **12**, 654.
- 65 P. S. Singh, K. Kosuge, V. Ramaswamy and B. S. Rao, *Appl. Catal., A*, 1999, **177**, 149.
- 66 S. Vetrival and A. Pandurangan, *Appl. Catal., A*, 2004, **264**, 243.
- 67 Y. Wang, Y. Chang, R. Wang and F. Zha, *J. Mol. Catal. A: Chem.*, 2000, **159**, 31.
- 68 (a) N. K. Mal and A. V. Ramaswamy, *Appl. Catal., A*, 1996, **143**, 75; (b) K. O. Xavier, J. Chacko and K. K. M. Yusuff, *J. Mol. Catal. A: Chem.*, 2002, **178**, 275; (c) K. O. Xavier, J. Chacko and K. K. M. Yusuff, *Appl. Catal., A*, 2004, **258**, 251; (d) T. H. Bennur, D. Srinivas and S. Sivasanker, *J. Mol. Catal. A: Chem.*, 2004, **207**, 163.
- 69 (a) M. R. Maurya, I. Jain and S. J. J. Titinchi, *Appl. Catal., A*, 2003, **249**, 139; (b) M. R. Maurya, A. Kumar, P. Manikandan and S. Chand, *Appl. Catal., A*, 2004, **277**, 45.
- 70 (a) K. J. Balkus, Jr. and A. G. Gabrielov, *J. Inclusion Phenom. Mol. Recognit. Chem.*, 1989, **21**, 159; (b) R. Raja and P. Ratnasamy, *Stud. Surf. Sci. Catal.*, 1996, **101**, 181; (c) C. R. Jacob, S. P. Varkey and P. Ratnasamy, *Appl. Catal., A*, 1998, **168**, 353; (d) C. R. Jacob, S. P. Varkey and P. Ratnasamy, *Microporous Mesoporous Mater.*, 1998, **22**, 465; (e) S. S. Deshpande, D. Srinivas and P. Ratnasamy, *J. Catal.*, 1999, **188**, 261; (f) S. Chavan, D. Srinivas and P. Ratnasamy, *J. Catal.*, 2000, **192**, 286; (g) M. R. Maurya, M. Kumar, S. J. J. Titinchi, H. S. Abbo and S. Chand, *Catal. Lett.*, 2003, **8**, 97; (h) M. R. Maurya, H. Saklani, A. Kumar and S. Chand, *Catal. Lett.*, 2004, **93**, 121.
- 71 G. Bellussi and G. Perego, in *Handbook of Heterogeneous Catalysis*, ed. G. Ertl, H. Knozinger and J. Weitkamp, Wiley, Poitiers, 1977, vol. 5, p. 2329.
- 72 R. M. Tóltaro, P. A. M. Williams, M. C. Apella, M. A. Blesa and E. J. Baran, *J. Chem. Soc., Dalton Trans.*, 2000, 4403.
- 73 (a) M. R. Maurya, S. Agarwal, C. Bader and D. Rehder, *Eur. J. Inorg. Chem.*, 2005, 147; (b) M. R. Maurya, S. Agarwal, C. Bader, M. Ebel and D. Rehder, *Dalton Trans.*, 2005, 537.
- 74 O. Bortolini, M. Bortolini, V. Conte and S. Moro, *Eur. J. Inorg. Chem.*, 2003, 42.